Discovery of simplified benzazole fragments derived from the marine benzosceptrin B as necroptosis inhibitors involving the receptor interacting protein Kinase-1

Mohamed Benchekroun, Ludmila Ermolenko, Minh Quan Tran, Agathe Vagneux, Hristo Nedev, Claire Delehouzé, Mohamed Souab, Blandine Baratte, Béatrice Josselin, Bogdan Iorga, et al.

Discovery of Simplified Benzazole Fragments Derived From The Marine Benzosceptrin C as Necroptosis Inhibitors Involving The Receptor Interacting Protein Kinase-1

Mohamed Benchekroun,[†] Ludmila Ermolenko,[†] Minh Quan Tran,[†] Agathe Vagneux,[†] Hristo Nedev,[†] Claire Delehouzé,[‡,‖] Mohamed Souab,[#] Blandine Baratte,[#] Béatrice Josselin [#] Bogdan I. Iorga,[†] Sandrine Ruchaud,[‖] Stéphane Bach,[‖,#,*] and Ali Al-Mourabit[†,*]

[†] Université Paris-Saclay, CNRS, Institut de Chimie des Substances Naturelles, Gif-sur-Yvette, 91190, France

[‡] SeaBeLife Biotech, Place Georges Teissier, 29680 Roscoff, France

[‖] Sorbonne Université, CNRS, UMR 8227, Integrative Biology of Marine Models Laboratory (LBI2M), Station Biologique de Roscoff, CS 90074, 29680 Roscoff, France

[#] Sorbonne Université, CNRS, FR 2424, Plateforme de criblage KISSf (Kinase Inhibitor Specialized Screening facility), Station Biologique de Roscoff, CS 90074, 29680 Roscoff, France

* Corresponding authors.
E-mail addresses: bach@sb-roscoff.fr (S. Bach), ali.almourabit@cnrs.fr (A. Al-Mourabit)

Highlights

- Design, synthesis of Benzosceptrin C-derived compounds as new necroptosis inhibitors.
- SAR study on the 54 benzazoles on the TNF-α induced necroptosis in human Jurkat FADD-deficient cells.
- Compounds **AV123** (**12**) and **MBM105** (**67**) inhibited RIPK1 with IC_{50} values of 12.12 and 2.89 μM, respectively.
- Potent, non-toxic and selective **MBM105** (**67**) blocked the necroptotic but not the apoptotic cell death.

Abstract

With the aim to develop new chemical tools based on simplified natural metabolites to help deciphering the molecular mechanism of necroptosis, simplified benzazole fragments including 2-aminobenzimidazole and the 2-aminobenzothiazole analogs were prepared during the synthesis of the marine benzosceptrin C. Conpounds inhibiting the RIPK1 protein kinase were discovered. A library of 54 synthetic analogues were prepared and evaluated through a phenotypic screen using the inhibition of the necrotic cell death induced by TNF-α in human

Jurkat T cells deficient for the FADD protein. This article reports the design, synthesis and biological evaluation of a series of 2-aminobenzazoles on the necroptotic cell death through the inhibition of RIPK1 protein kinase. The 2-aminobenzimidazole and 2-aminobenzothiazole platforms presented herein can serve as novel chemical tools to study the molecular regulation of necroptosis and further develop lead drug candidates for chronic pathologies involving necroptosis.

1. Introduction

The regulation of cell death is crucial for the homeostasis control for all living beings. The concept of programmed cell death (PCD), that emerged early in the 1960s, referred to the sequence of molecular events that lead to death of the cell.[1] This physiological process, which occurs in the absence of any exogenous perturbations, is notably essential for the development of multicellular organisms and for maintaining the tissue homeostasis in the whole organism. The "regulated cell death" (RCD) was then introduced to define the molecular processes that were initiated from perturbations of intracellular or extracellular micro-environment, when adaptive responses are incapable of restoring cellular homeostasis. As defined by the Nomenclature Committee on Cell Death (NCCD), the major RCD subroutines includes extrinsic and intrinsic apoptosis, entotic cell death, NETotic cell death, lysosome-dependent cell death, autophagy-dependent cell death, immunogenic cell death, mitotic death, pyroptosis, parthanatos, mitochondrial permeability transition (MPT)-driven necrosis, ferroptosis and necroptosis.[2]

Necroptosis is a RCD that has attracted increasing consideration regarding its involvement in numerous pathologies including ischemia-reperfusion injuries (including stroke, myocardial infarction, resuscitation, solid organ transplantation or heart surgery) in brain, heart and kidney, inflammatory diseases, sepsis, retinal disorders, neurodegenerative diseases, infectious disorders and liver disease.[3–5] Necroptosis may be activated upon stimulation by the cytokines TNF-α (Tumor Necrosis Factor-α), FasL (Fas Ligand) and TRAIL (tumor-necrosis-factor related apoptosis inducing ligand) and relies on the activity of two serine-threonine kinases, RIPK1 (Receptor-Interacting Protein Kinase-1) and RIPK3, and on the pseudo-kinase MLKL (Mixed Lineage Kinase domain-Like). After the stimulation of receptors by the corresponding cytokines, necroptosis may occur under apoptotic deficient

conditions: e.g. deficiency in caspase-8 or in Fas-Associated protein with Death Domain - FADD protein (see Zhou and Yuan, 2014, for review[6]). The enzymatic inhibition of caspases by zVAD.fmk was used in 2005 by Degterev et al. to identify the first small-molecule inhibitor of necroptosis, the necrostatin-1 (Nec-1, **1**).[7] Nec-1, bearing a methyl-thiohydantoin-tryptophan (MTH-Trp) scaffold, was characterized in a phenotypic screen for small-molecules able to inhibit the necrotic cell death induced by TNF-α in human monocytic U937 cells. The chlorinated analogue of Nec-1, Nec-1s (**2**), was then described to be endowed with a better pharmacokinetic profile, an increased specificity for RIPK1 over a broad range of kinases and an absence of indoleamine-2,3-dioxygenase (IDO)- inhibitory activity.[8] Necrostatins served as privileged tools to better understand the necroptosis cascade. However, their development as drugs was hampered due especially to poor SAR profile as well as unfavorable pharmacokinetic factors.[9]

Following the necrostatins, several inhibitors of necroptosis were subsequently described over the last decade.[10] Representative examples are given in Figure 1. For instance, GSK has disclosed a chemical series of benzo[*b*][1,4]oxazepin-4-one analogs [11] that proved to be effective anti-necroptosis agents.[12] Among them, the clinical candidate GSK2982772 (**3**) completed the phase 2 clinical studies for psoriasis, rheumatoid arthritis, and ulcerative colitis.[13] Subsequently, Takeda researchers have discovered new brain-penetrating necroptosis inhibitors based on the benzo[*b*][1,4]oxazepin-4-one core of lead compound **3**. Subsequently, lead optimization efforts furnished compound **4** having a potent cellular anti-necroptotic action *in vitro* for the treatment of neurodegenerative diseases. Moreover, compound **4** was able to significantly diminish disease progression in an experimental autoimmune encephalomyelitis (EAE) murine model of multiple sclerosis.[14] In order to find additional chemotypes, Harris et al. initiated a high throughput screen on the GSK compound collection to identify novel inhibitors targeting the allosteric binding site in RIPK1. This has led to the discovery of the 4,5-dihydropyrazole GSK963 (**5**) [15] which furnished after lead optimization efforts compounds **6** and **7**, orally bioavailable and highly selective RIPK1 inhibitors.[16] Following an original drug repurposing strategy,[17] Augustyns and colleagues have devised a series of new Tozasertib analogs as inhibitors of necroptotic cell death. Tozasertib is a Type I pan-Aurora kinase inhibitor that was also found to inhibit the mTNF-induced necroptosis. Interestingly, compound **8** did not inhibit the Aurora

kinases while strongly inhibiting RIPK1. Compound **8** was also potent *in vivo* in a TNF-induced systemic inflammatory response syndrome (SIRS) mouse model.[18] Finally, one of us and colleagues screened a kinase-focused library and discovered 4-(1*H*-pyrrolo[2,3-*b*]pyridin-2-yl)phenol (**9**), dubbed Sibiriline, as a new RIPK1 inhibitor. Sibiriline was shown to protect mice from immune-mediated acute hepatitis by significantly decreasing serum aspartate aminotransferase (AST) and alanine amino transferase (ALT) levels and liver injury. [4]

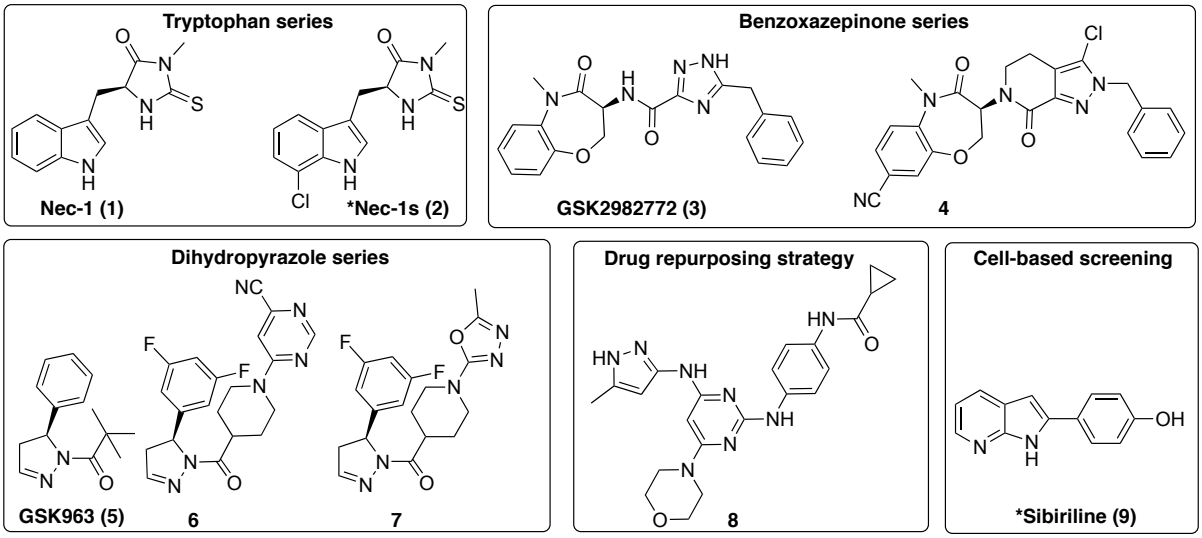

Figure 1. Chemical structures of selected inhibitors of necroptosis. * Nec-1s (**2**) and Sibiriline (**9**) were used as controls in this study.

Therefore, substantial breakthroughs in the knowledge of the medicinal chemistry of necroptosis through the discovery of new-programmed cell death inhibitors or activators are expected not only to lead to original and effective drugs, but also to decipher various molecular mechanisms involved in PCD pathways. Taking into account these latter developments and our interest in necroptotic cell death mechanisms using kinase inhibitors as molecular probes, we recently turned our attention to marine natural products and their simplified fragments. Of particular interest, some marine metabolites bearing the 2-aminoimidazole or the 2-aminobenzimidazole moieties were found to modulate the enzymatic activity of several kinases. For example, the marine natural product 10*Z*-hymenialdisine showed potent activity on several serine/threonine kinases such as GSK-3β, CDK1 (cyclin-dependent kinase 1), CDK2, CDK5, CK1 (casein kinase-1) and MAPKK-1 (Mitogen-activated protein kinase kinase 1) that are involved in the cell life cycle.[19]

In a synthetic project targeting the total synthesis of the marine Benzosceptrin C (**10**) [20] that inhibits kinase CK1δ with an IC_{50} of 0.68 µM, we explored the kinase activity of several truncated fragments based on the 2-aminobenzimidazole sub-structure. Indeed, structural simplification of natural products is nowadays a well-established strategy to circumvent limitations such as narrow synthetic accessibility, unfavorable pharmacokinetics and poor drug-likeness.[21,22]

In this study, we used the FADD-deficient Jurkat T cells treated with 10 ng/mL human TNF-α as in vitro model of necroptosis induction. As described in Delehouzé et al., this forward chemical biology approach can be used to screen chemical libraries for characterization of RIPK1 inhibitors.[5] Among the various simplified fragments of benzosceptrin C we have screened (undisclosed results), compound **AV123** (**12**) demonstrated a clear inhibition of TNF-α induced necroptosis with an EC_{50} of 1.7 µM, highlighting the simple benzazole core as a promising chemical platform for necroptosis and RIPK1 inhibition. The goal of this study was to identify further benzosceptrin C-inspired fragments that are easy to diversify in order to evaluate RIPK1 as a key target in necroptosis inhibition. We therefore launched a medicinal chemistry project aimed at finding further necroptosis inhibitors based on the 2-aminobenzazole scaffold of the hit compound **AV123** (**12**) (Figure 2). We show herein that: (i) RIPK1 is targeted by the more potent hits; (ii) these new RIPK1 inhibitors were shown to block necroptotic but not apoptotic cell death.

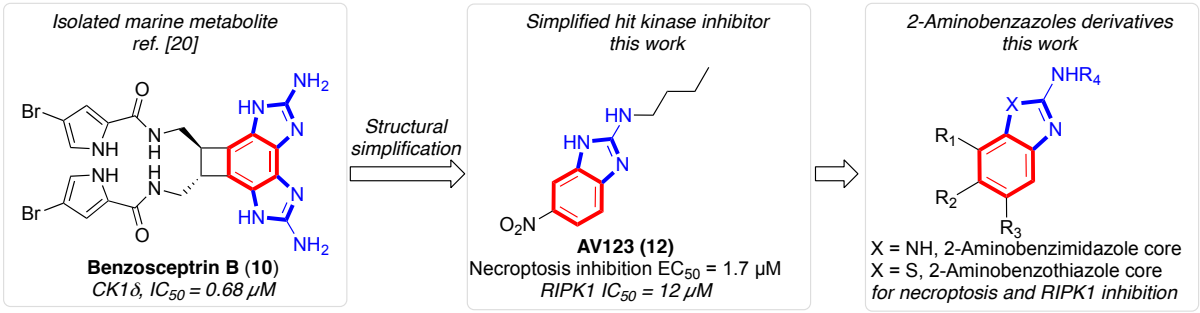

Figure 2. Chemical structures of benzosceptrin B (**10**), hit compound **AV123** (**12**) and the general structure of the 2-aminobenzazole derivatives targeted in this work.

2. Results and discussion

2.1. Chemistry

Initially, we were concerned that the structural complexity of the kinase inhibitor benzosceptrin C make it unsuitable for further development. Thus, we decided to further explore the simplified hit compound **AV123** (**12**) and its 2-aminobenzimidazole analogs **13-49** that were prepared according to two standard procedures (Scheme 1 and Table 1). The first procedure involves the reaction of 2-aminobenzimidazoles **10a-k** with selected isothiocyanates in presence of a desulfurization reagent such as dicyclohexylcarbodiimide (DCC) or diisopropylcarbodiimide (DIC) in acetonitrile. The second procedure involves the reaction of diaminoarenes **11b**, **11f** and **11g** with selected commercially available isocyanides in presence of a catalytic amount of elemental selenium. Compounds were obtained in overall satisfactory yields (Table 1).

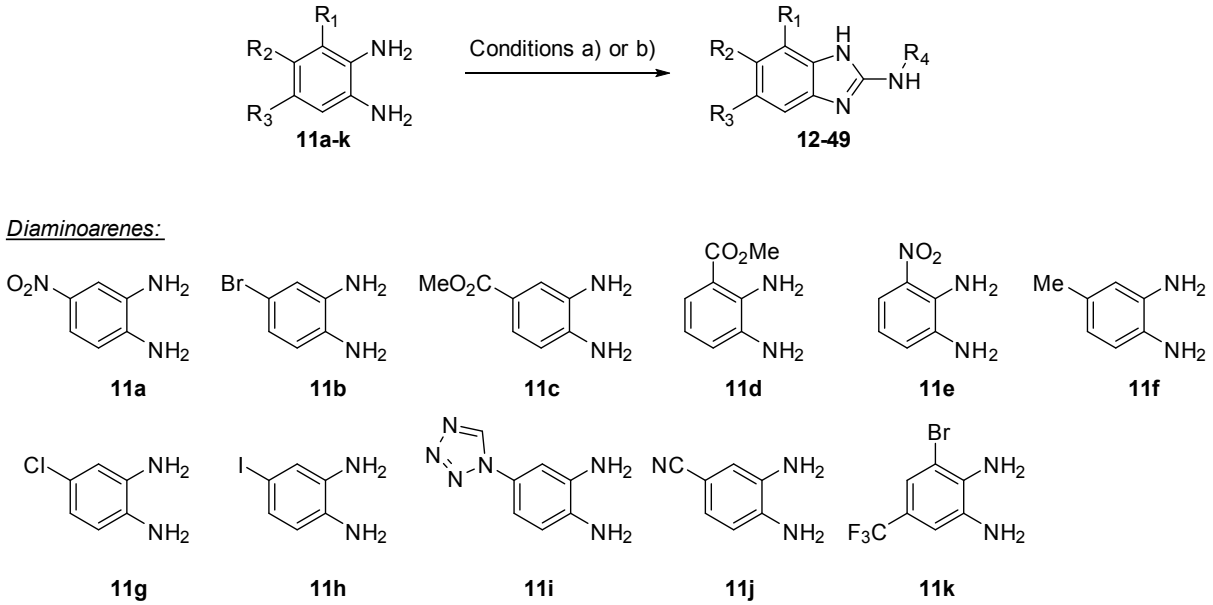

Scheme 1. *Reagents and conditions:* a) 1.2 equiv. R_4NCS, 1.2 equiv. dialkylcarbodiimide, ACN or Py, 80°C, 16h; b) 1.5 equiv. R_4NC, 1 mol% Se powder, Py, 90-110°C, 24h.

Table 1. Yields of 2-aminobenzimidazoles **12 - 49.**

Diaminoarene	R_1	R_2	R_3	R_4	Benzimi-dazole	yield
11a	H	NO_2	H	*n*Bu	**AV123 (12)**	90%[a]
11a	H	NO_2	H	Et	**13**	70%[a]

11a	H	NO_2	H	*n*Pr	**14**	48%[a]
11a	H	NO_2	H	*n*Hex	**15**	74%[a]
11a	H	NO_2	H	*n*Oct	**16**	58%[a]
11a	H	NO_2	H	*i*Pr	**17**	92%[a]
11a	H	NO_2	H	Allyl	**18**	80%[a]
11a	H	NO_2	H	Propargyl	**19**	26%[a]
11a	H	NO_2	H	*sec*Bu	**20**	24%[a]
11a	H	NO_2	H	Methoxyethyl	**21**	36%[a]
11a	H	NO_2	H	*c*Hex	**22**	66%[a]
11a	H	NO_2	H	Ph	**23**	78%[a]
11a	H	NO_2	H	Bn	**24**	66%[a]
11a	H	NO_2	H	Bz	**25**	70%[a]
11a	H	NO_2	H	*p*-Br-Ph	**26**	43%[a]
11a	H	NO_2	H	*p*-CN-Ph	**27**	87%[a]
11a	H	NO_2	H	*p*-CF_3-Ph	**28**	35%[a]
11a	H	NO_2	H	*p*-NO_2-Ph	**29**	87%[a]
11a	H	NO_2	H	*p*-$N(Me)_2$-Ph	**30**	70%[a]
11a	H	NO_2	H	CH_2CO_2Et	**31**	49%[a]
11b	H	Br	H	Et	**32**	39%[a]
11b	H	Br	H	*n*Bu	**33**	46%[a]
11c	H	CO_2Me	H	*n*Bu	**34**	82%[a]
11d	CO_2Me	H	H	*n*Bu	**35**	83%[a]
11d	CO_2Me	H	H	*c*Hex	**36**	56%[b]
11e	NO_2	H	H	*i*Pr	**37**	95%[a]
11e	NO_2	H	H	*n*Bu	**38**	95%[a]
11e	NO_2	H	H	Methoxyethyl	**39**	84%[a]
11e	NO_2	H	H	*c*Hex	**40**	50%[a]
11e	NO_2	H	H	Ph	**41**	96%[a]
11e	NO_2	H	H	Bn	**42**	73%[a]

11f	H	Me	H	*c*Hex	**43**	74%[b]
11g	H	Cl	H	*c*Hex	**44**	82%[b]
11b	H	Br	H	*c*Hex	**45**	70%[b]
11h	H	I	H	*n*Bu	**46**	43%[a]
11i	H	1λ²-tetrazolyl	H	*n*Bu	**47**	48%[a]
11j	H	CN	H	*n*Bu	**48**	14%[a]
11k	Br	H	CF_3	*n*Bu	**49**	39%[a]

[a] Prepared according to condition a) in Scheme 1; [b] Prepared according to condition b) in Scheme 1.

Substituent effects on the phenyl ring of **AV123** were then examined. For this purpose, the nitro group found in the R_2 position of **AV123** was replaced by aryl substituents. Compounds **50-55** (Scheme 2) were prepared from the above brominated compounds **32-33** and selected commercially available boronic acids using the Suzuki-Miyaura cross-coupling reaction. Two conditions palladium/base combinations were used ($Pd(PPh_3)_4/K_2CO_3$ or $PdCl_2(dtbpf))/K_3PO_4$ in 1,4-dioxane/water : 1/0.1).

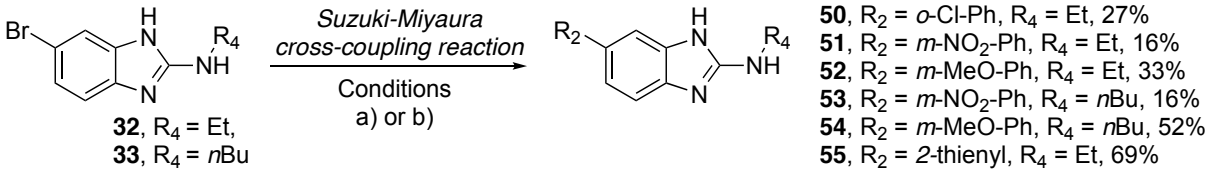

Scheme 2. *Reagents and conditions*: a) $R_2B(OH)_2$ (1 equiv.), K_2CO_3 (3 equiv.), $Pd(PPh_3)_4$ (5 mol%, 0.02 mmol), 1,4-dioxane/water: 1/0.1, 16h; b) $R_2B(OH)_2$ (1 equiv.), K_2CO_3 (3 equiv.), (5 mol%, 0.02 mmol), 1,4-dioxane/water: 1/0.1, 16h.

The triazolyl-containing compound **58** was obtained through the acetylenic intermediate **57** (Scheme 3). First, a Sonogashira cross-coupling reaction between the brominated compound **33** and trimethylsilylacetylene furnished the silylated acetylenic intermediate **56** which was subsequently desilylated to furnish **57** which was subsequently treated with benzyl azide then $CuSO_4.5H_2O$/sodium ascorbate to give **58** in a one-pot fashion.

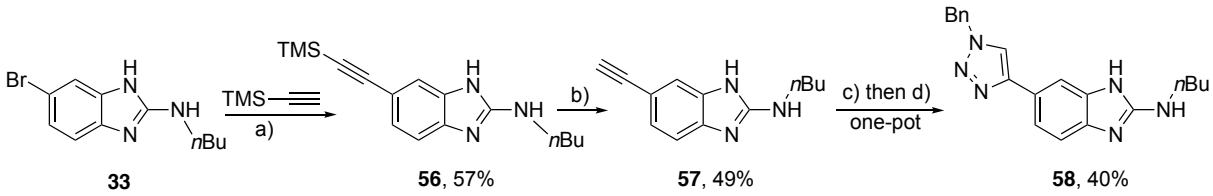

Scheme 3. *Reagents and conditions:* a) 10 mol% $PdCl_2$(dtbpf) (0.10 equiv.), 20 mol% (CuI (0.20 mmol) TEA (5 equiv.), dry DMF (0.5 mL); b) K_2CO_3 (1.1 equiv.), MeOH/water 1:1; c) BnN_3 (1.1 equiv.), DMF/water: 1/0.2, 16h; d) 10 mol% $CuSO_4.5H_2O$ (0.1 equiv.), 20 mol% Na ascorbate (0.2 equiv.), 16h.

Selected 2-aminobenzimidazole esters **31** and **34** (Scheme 4) were directly coupled with appropriate amines using 1,5,7-triazabicyclo[4.4.0]dec-5-ene (TBD), as an activator of the ester functionality, in acetonitrile to give the amides **59-63**.

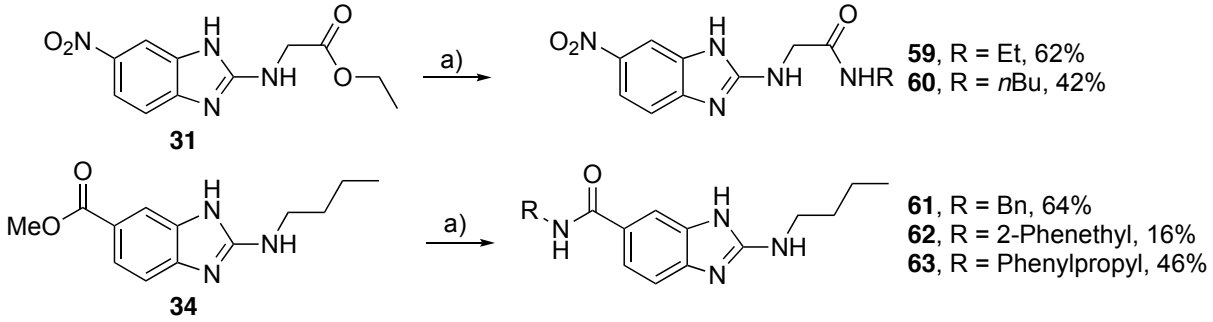

Scheme 4. *Reagents and conditions*: a) TBD (1 equiv.), amine (5 equiv.), ACN or neat.

The reaction of the commercially available 2-chlorobenzothiazoles **64** and **65** with *n*-butylamine in the presence of DBU and $NaHCO_3$ afforded the corresponding 2-aminobenzothiazoles regioisomers **66** and **67** in good yields (Scheme 5).[23]

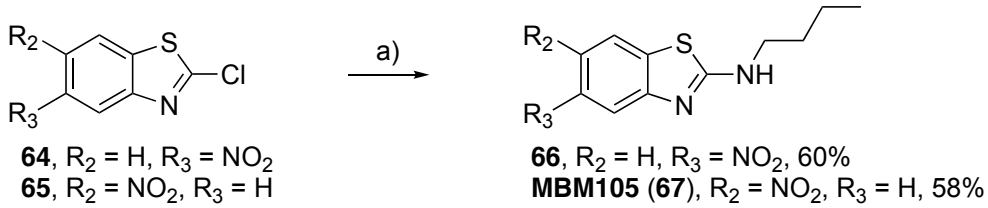

Scheme 5. *Reagents and conditions*: a) DBU, *n*$BuNH_2$, $NaHCO_3$, neat.

2.2. Biological results

2.2.1. Characterization of the 2-aminobenzazole derivatives as new inhibitors of necroptosis

To evaluate the antinecroptotic activity of the selected compounds, the regulated necrosis was induced by TNF-α in human FADD-deficient Jurkat T cells resistant to extrinsic apoptosis (Table 2). Structure-activity relationships studies revealed that only few modifications were tolerated at the R_1, R_2, R_3 and R_4 positions of the benzimidazole core. For instance, a complete loss of necroptotic activity was observed when replacing the nitro group at R_2 by any aryl/heteroaryl (compounds **47**, **50**, **51**, **52**, **53**, **54**, **55**, **56**, **58**), ester (compound **34**), amide (compounds **61-63**) or alkynyl groups (compounds **56** and **57**). Nevertheless, compound **44** bearing a chloro- substituent and **48** bearing a cyano substituent at R_2 showed an EC_{50} of 4.4 μM and 8.9 μM, respectively. Varying the substitution at R_4 while fixing R_1 = H, R_2 = NO_2 and R_3 = H, showed that the *n*-butyl found in **AV123 (12)** or the *sec*-butyl groups in compound compound **20** were the most promising compounds. Moreover, the switch from the 2-aminobenzimidazole to the 2-aminobenzothiazole nucleus proved to be beneficial for the anti-necroptotic activity. Indeed, the structurally related benzothiazoles **66** (R_1 = H, R_2 = NO_2, R_3 = H, R_4 = *n*Bu) and **MBM105** (**67**) (R_1 = H, R_2 = H, R_3 = NO_2, R_4 = *n*Bu) showed an EC_{50} of 6.9 and 4.7 μM, respectively. As a result, the 2-aminobenzimidazole **AV123** and the 2-aminobenzothiazole **MBM105** (**67**) emerged as promising hit molecules. They are potent inhibitors of cell-death phenotype but also poorly toxic. Four other compounds, namely **20**, **22**, **23** and **44**, were also shown to be potent inhibitors of necroptosis but they are toxic when used above 10 μM concentration (see supplementary Figure 1 in Supporting Information for details). Even if **AV123** inhibited the cell viability of FADD-deficient Jurkat cells at the highest doses tested (> 25μM), we decided to select this compound because it emerged as the most potent inhibitor of necroptosis (EC_{50}= 1.7 μM). The ability of the selected molecules to inhibit necroptosis was also compared to known inhibitors of RIPK1 kinase, Nec-1s and Sibiriline.

Table 2. Primary cell-based screening on the TNF-α-induced necroptosis in Jurkat FADD deficient cells.[a]

Cmpd	X	R_1	R_2	R_3	R_4	ProtecΔ at 10µM	EC_{50} (µM)
AV123 (12)	NH	H	NO_2	H	*n*Bu	**56.9**	**1.7**
13	NH	H	NO_2	H	Et	6.4	ND
14	NH	H	NO_2	H	*n*Pr	**20**	**14.4**
15	NH	H	NO_2	H	*n*Hex	23.6	ND[b]
16	NH	H	NO_2	H	*n*Oct	6.4	ND
17	NH	H	NO_2	H	*i*Pr	**16.2**	**> 25**
18	NH	H	NO_2	H	Allyl	4.7	ND
19	NH	H	NO_2	H	Propargyl	3.4	ND
20	NH	H	NO_2	H	*sec*Bu	**53.7**	**2.2**
21	NH	H	NO2	H	Methoxyethyl	5.6	ND
22	NH	H	NO_2	H	*c*Hex	**68.1**	**1.04**
23	NH	H	NO_2	H	Ph	**41.9**	**2.5**
24	NH	H	NO_2	H	Bn	9	ND
25	NH	H	NO_2	H	Bz	-21.3	ND
26	NH	H	NO_2	H	*p*-Br- Ph	-6.1	ND
27	NH	H	NO_2	H	*p*-CN- Ph	-31.4	ND
28	NH	H	NO_2	H	*p*-CF_3- Ph	-30.8	ND
29	NH	H	NO_2	H	*p*-NO_2- Ph	3.6	ND
30	NH	H	NO_2	H	*p*-$(NMe)_2$-Ph	14.0	ND
31	NH	H	NO_2	H	CH_2CO_2Et	15.3	ND
32	NH	H	Br	H	Et	10.4	ND
33	NH	H	Br	H	*n*Bu	7.3	ND
34	NH	H	CO_2Me	H	*n*Bu	2.9	ND
35	NH	CO_2Me	H	H	*n*Bu	**29.2**	**18.1**
36	NH	CO_2Me	H	H	*c*Hex	**21.7**	**9**[c]
37	NH	NO_2	H	H	*i*Pr	1	ND

38	NH	NO_2	H	H	*n*Bu	1.2	ND
39	NH	NO_2	H	H	Methoxyethyl	-2.3	ND
40	NH	NO_2	H	H	*c*Hex	13.0	ND
41	NH	NO_2	H	H	Ph	0	ND
42	NH	NO_2	H	H	Bn	5.1	ND
43	NH	Me	H	H	*c*Hex	**7**	ND
44	NH	H	Cl	H	*c*Hex	**38.2**	**4.4**
45	NH	H	Br	H	*c*Hex	43.7	ND[b]
46	NH	H	I	H	*n*Bu	-16.3	ND
47	NH	H	H	H	*t*Bu	-1.32	ND
48	NH	H	1λ²-tetrazolyl	H	*n*Bu	6.3	
49	NH	H	CN	H	*n*Bu	**23.7**	**8.9**
50	NH	Br	H	CF_3	*n*Bu	4.9	ND
51	NH	H	*o*-Cl-Ph	H	Et	-19.4	ND
52	NH	H	*m*-NO_2-Ph	H	Et	-12.8	ND
53	NH	H	*m*-MeO-Ph	H	Et	-20.6	ND
54	NH	H	*m*-NO_2-Ph	H	*n*Bu	-16.8	ND
55	NH	H	*m*-MeO-Ph	H	*n*Bu	-20.5	ND
56	NH	H	2-Thienyl	H	*n*Bu	-18.5	ND
57	NH	H	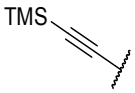	H	*n*Bu	-21.3	ND
58	NH	H		H	*n*Bu	-10.5	ND
59	NH	H	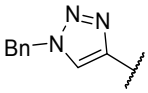	H	*n*Bu	1.9	ND
60	NH	H	NO_2	H	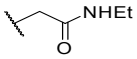	4.6	ND
61	NH	H	NO_2	H	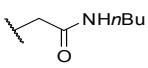	5.0	ND
62	NH	H	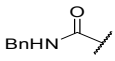	H	*n*Bu	2.6	ND

63	NH	H	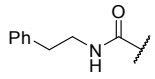	H	*n*Bu	-3.6	ND
64	NH	H	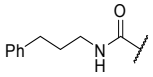	H	*n*Bu	0.1	ND
66	S	H	NO_2	H	*n*Bu	**28.0**	**6.9**
MBM105 (**67**)	S	H	H	NO_2	*n*Bu	**56.1**	**4.7**
Sibiriline (**9**)						**57.9**	**1.1**

[a] The table displays the % of remaining viable cells after co-treatment with 10 µM of the tested compound and with TNF-α (10 ng/ml). Cell viability was measured by MTS reduction assay as mentioned in the Experimental part section. The values were normalized, considering 100 % viable cells in the control treated only with DMSO (n = 3). The level of protection against the TNF-α-induced cell death of each tested compounds is estimated using the "protection delta" (ProtecΔ) values. These values are determined by subtracting the smaller number (value obtained with TNF-α and without the tested compound) from the larger one (value obtained for co-treatment with TNF-α and with the tested compound). In some cases, the tested compounds can be toxic and thus we may have to subtract the larger one from the smaller one. This might result in a negative number. The EC_{50} of the more effective molecules (ProtecΔ>16) were determined from the dose-response curves using Graphpad PRISM software (data are mean, n = 3). ND, not determined.

[b] A treatment with more than 10 µM of compounds **15** and **45** compound decreased strongly the viability of Jurkat FADD deficient cells. It was thus impossible to determine an EC_{50} value for this compound.

[c] A treatment with more than 25 µM of compound **36** was shown to have a negative effect on the viability of Jurkat FADD deficient cells that could correspond to a toxic effect. Nevertheless, it was possible to calculate an EC_{50} from the dose-response curve.

As shown on Figure 3, panel **A**, **AV123 (12)** and **MBM105** (**67**) efficiently blocked necroptosis in a dose-dependent manner, and with an efficacy almost similar to Sibiriline. Moreover, cell viability analysis of retina cell line grown in presence of **AV123 (12)** and **MBM105** (**67**) for 24 hours indicated that none of the two compounds exhibited toxicity to RPE-1 cells at concentrations from 0.01 to 50 µM (Figure 2, panel **B**). The bioactivities of **AV123 (12)** and **MBM105** (**67**) were studied in the work reported here.

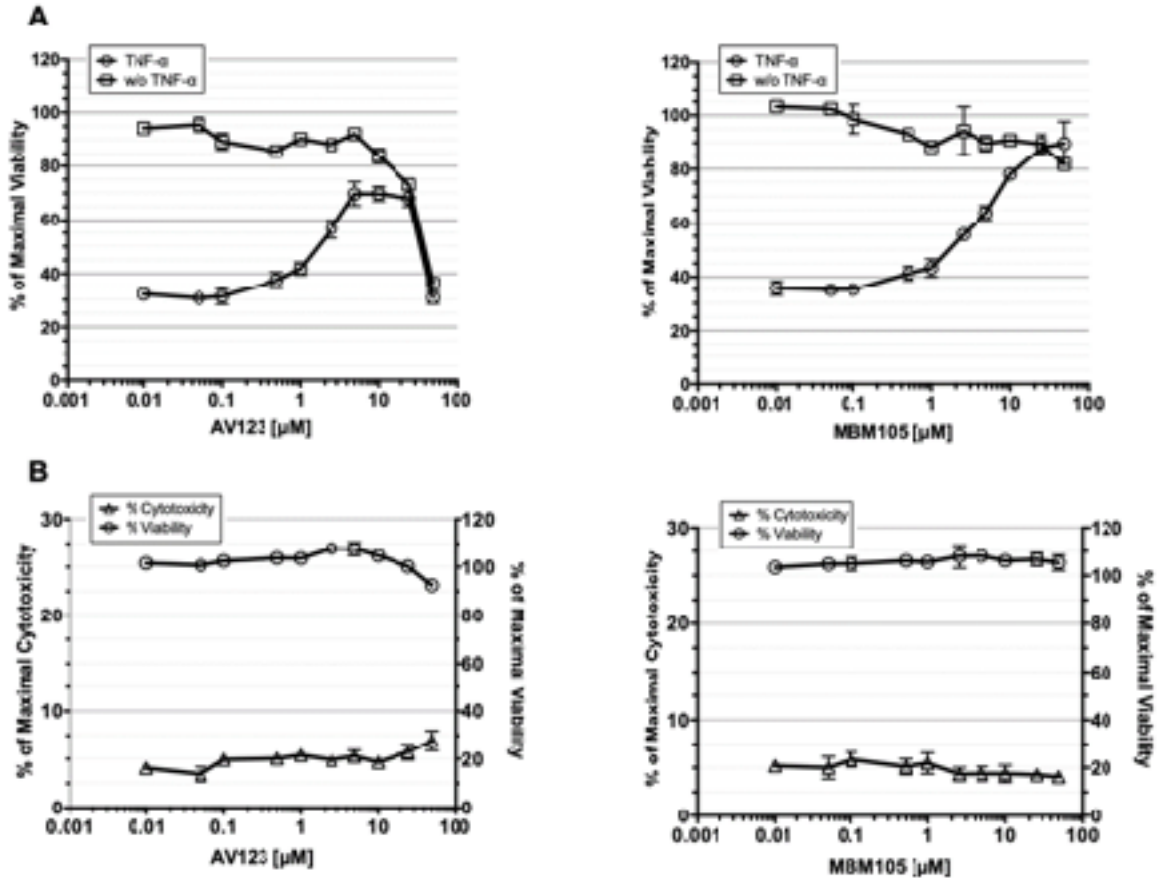

Figure 3. Dose-dependent inhibition of TNF-α-induced necroptosis by increasing concentrations of **AV123 (12)** and **MBM105** (**67**). (A) After a 24-h incubation of Jurkat FADD deficient cells with or without (w/o) 10 ng/ml TNF-α and increasing concentrations of tested compounds. The effect of the co-treatment on the cell viability was evaluated by MTS reduction assay. Treatments without TNF-α were used to estimate the toxicity of the tested compound. The values were normalized as a percentage of cell viability, considering 100% viable cells in the control treated with DMSO (n = 3, mean ± SD). (B) Evaluation of the toxicity of **AV123 (12)** and **MBM105** (**67**) on hTERT-immortalized retinal pigment epithelial cell line, hTERT RPE-1. RPE-1 retina cells were exposed for 24-hours to increasing concentrations of the tested compound (ranging from 0.01 to 50 µM). Cell viability was assessed and plotted as mentioned here above. A similar experiment was performed to measure cellular death (LDH release assay; left axis). Results are plotted in % of maximal LDH release (cell lysis). Data are mean ± SD (n= 3).

2.2.2. AV123 (12) and MBM105 (67) are inhibitors of human RIPK1

In order to decipher the mechanism of action of **AV123 (12)** and **MBM105** (**67**), the RIPK1 enzymatic activity was monitored in the presence of the compounds. The catalytic activity of RIPK1 was quantified by monitoring the phosphorylation of myelin basic protein (MBP), a known substrate of RIPK1 (KinaseProfiler™ assay, Eurofins Discovery, Celle-L'Evescault, France). As shown in Figure 4, **AV123 (12)** and **MBM105** (**67**) efficiently inhibit the phosphorylation of MBP by RIPK1 in a dose-dependent manner with IC_{50} equal to 12.12 and 2.89 µM, respectively. The inhibition of the enzymatic activity by **AV123 (12)** was also observed using an in vitro auto-phosphorylation assay using recombinant full-length RIPK1 (GST-tagged). This assay showed an inhibition of RIPK1 auto-phosphorylation by **AV123 (12)** in a dose-dependent manner. Taken altogether, these data demonstrated that the selected molecules **AV123 (12)** and **MBM105** (**67**) are inhibitors of RIPK1 kinase activity. In a recent paper, a RIPK1 inhitor including similar benzothiozole motif was described.[24]

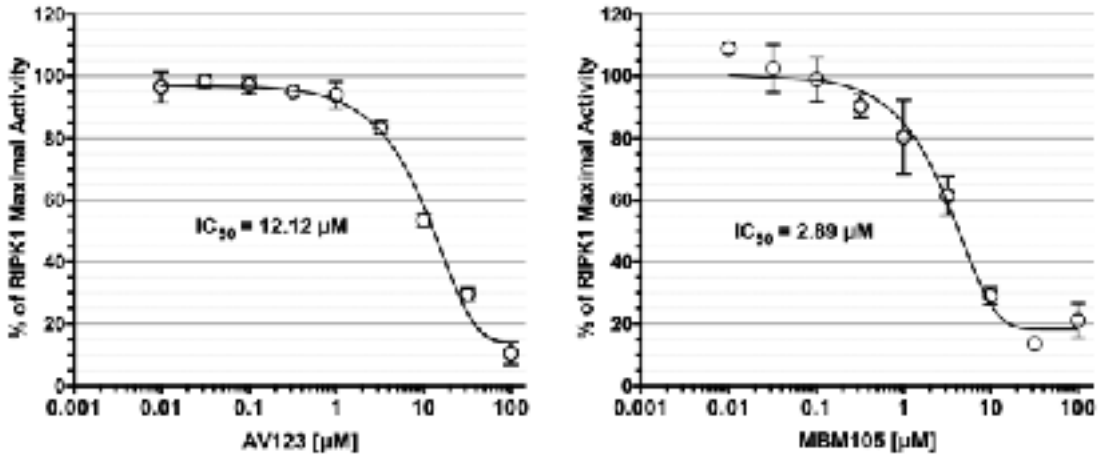

Figure 4. Effects of **AV123 (12)** and **MBM105** (**67**) on the catalytic activity of RIPK1 kinase. RIPK1 was assayed in the presence of increasing concentrations (ranging from 0.01 to 100µM) of **AV123 (12)** and **MBM105** (**67**). ATP concentration used in the kinase assays was 155 µM. Kinase activities are expressed in % of RIPK1 maximal activity, i.e. measured with the same amount of DMSO and in the absence of inhibitor. Data are mean ± range, n= 2. We further evaluated the bioactivity of compounds **AV123 (12)** and **MBM105** (**67**) against a short panel of disease-related serine/threonine protein kinases: three human cyclin dependent kinases (CDK2/Cyclin A, CDK5/p25 and CDK9/Cyclin T), mouse CDC2-like kinase 1 (CLK1), rat dual specificity tyrosine-phosphorylation-regulated kinase 1A (DYRK1A),

human proto-oncogene PIM1, human Janus Kinase 3 (JAK3), human Abelson murine leukemia viral oncogene homolog 1 (ABL1), human mitotic kinases Haspin and Aurora B, casein kinase 1 isoform epsilon (CK1ε), receptor-interacting protein 3 (RIPK3). As reported on Table 3, **AV123 (12)** and **MBM105** (**67**) were shown to inhibit DYRK1A with IC_{50} of 1.80 and 2.21 μM, respectively. **AV123 (12)** was shown to be putatively less selective compared to **MBM105** (**67**) as **AV123 (12)** was also shown to inhibit CDK9/Cyclin T and CLK1 with sub-micromolar IC_{50} of 0.48 and 0.80 μM, respectively.

Table 3. Inhibitory activities of **AV123 (12)** and **MBM105** (**67**) against a short panel of disease-related protein kinases. The table displays the IC_{50} values determined from the dose-response curves. ATP concentration used in the kinase assays was 10 μM (values are means, n= 2). Kinases are from human origin unless specified: (*Mm*), *Mus musculus*; (*Rn*), *Rattus norvegicus*.

Cpd	CDK2/ CyclinA	CDK5/ p25	CDK9/ CyclinT	*(Mm)* CLK1	*(Rn)* DYRK 1A	HASPIN	Pim1	CK1ε	JAK3	ABL1	RIPK3	AURKB
AV123	> 10 μM	> 10 μM	**0.48**	**0.80**	**1.80**	> 10 μM	> 10 μM	> 10 μM	> 10 μM	> 10 μM	> 10 μM	> 10 μM
MBM105	> 10 μM	> 10 μM	> 10 μM	> 10 μM	**2.21**	> 10 μM	> 10 μM	> 10 μM	> 10 μM	> 10 μM	> 10 μM	> 10 μM

2.2.3. The more selective RIPK1 inhibitor, MBM105, blocks necroptotic but not apoptotic cell death

To further analyze the bioactivity of **MBM105** (**67**), we next tested its ability to inhibit apoptotic cell death. As shown by the results reported on Figure 4, **MBM105** (**67**) did not rescue WT Jurkat cells from death-receptor (DR)-induced apoptosis (induction by treatment with the cytokine TRAIL) or DR-independant induced apoptosis (induction by treatment with the pan-kinase inhibitor, Staurosporine, STS). In the same conditions, the pan-caspase inhibitor Z-VAD-fmk was shown to inhibit both ways of apoptosis induction. As STS is known to induce both caspase-dependent and caspase-independent cell-death modalities,[25] the inhibition of staurosporine-induced cell-death by Z-VAD-fmk was less potent compared to TRAIL-induced apoptosis (Figure 5). Note here that the specificity toward necroptosis was also observed for Sibiriline and necrostatin-1 by Le Cann et al.[4] Overall, these data indicate that the lead compound **MBM105** (**67**) is selective towards necroptosis.

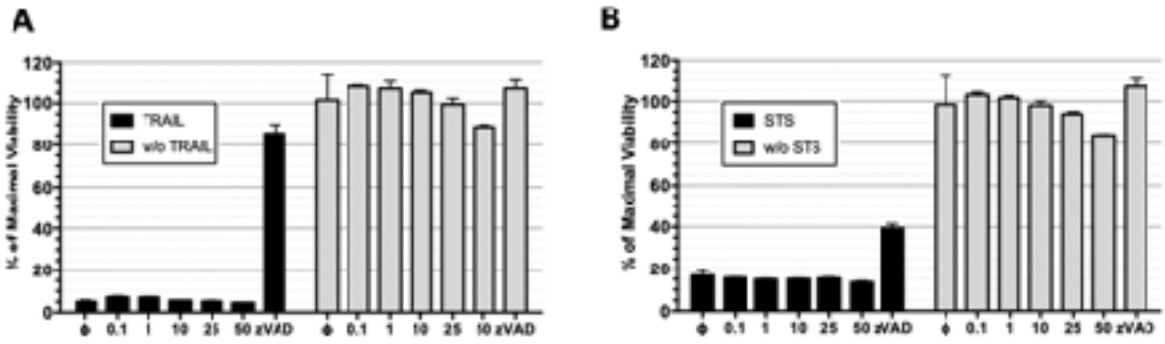

Figure 5. **MBM105** (**67**) does not inhibit TRAIL and staurosporine-induced apoptosis. Apoptosis was induced in Jurkat wild-type cells by treatment with either (panel A) TRAIL-Flag (20 ng.mL-1) or (panel B) staurosporine (STS, 100 nM). Cells were then simultaneously treated by increasing doses of **MBM105** (**67**) or Z-VAD-fmk (20 µM) as cell-permeant pan-caspase inhibitor. After a 24-h incubation, the effect of the tested compound on the cell viability was evaluated by MTS reduction assay and is expressed in % of survival in cells treated with DMSO. Data are mean ± SD (n= 3).

2.3. Molecular docking

The interaction of RIPK1 with representative inhibitors synthesized in this work was studied using molecular docking calculations. First, the reliability of our protocol was evaluated by docking the compound 2-benzyl-5-nitro-1*H*-benzimidazole in the binding site of RIPK1 (PDB code 6C3E).[14] As shown in Figure 6a, b; the docking conformation reproduces well the X-ray structure of the ligand, with a root-mean-square deviation (RMSD) of 0.59 Å. The ligand is stabilized by hydrogen bond interactions of N-3 with backbone NH of Asp156 and of NH-1 with backbone O of Val76, as well as mainly hydrophobic interactions between the phenyl ring and a subpocket defined by the side chains of residues Leu70, Val75, Ile154, Leu129, Val134, Phe162, Ser161, His136 and Asp156 (Figure 6a, b). Compound **AV123 (12)** binds in a similar manner, with the NH-nBu substituent in the hydrophobic pocket and the hydrogen bond of N-3 with backbone NH of Asp156 (Figure 6c, d). This latter interaction seems to control the global orientation of the ligand in the binding site, positioning the nitro group between the side chains of Leu90 and Met92, slightly shifted upwards compared with the reference ligand. The same conformation is observed for **MBM105** (**67**), again strongly influenced by the hydrogen bond of N-3 with backbone NH of Asp156 (Figure 6e,f). Overall,

these complexes show a very good shape complementarity between the protein and the ligand (Figure 6a, c, e), with a good tolerance of the nitro group in the positions 5 and 6.

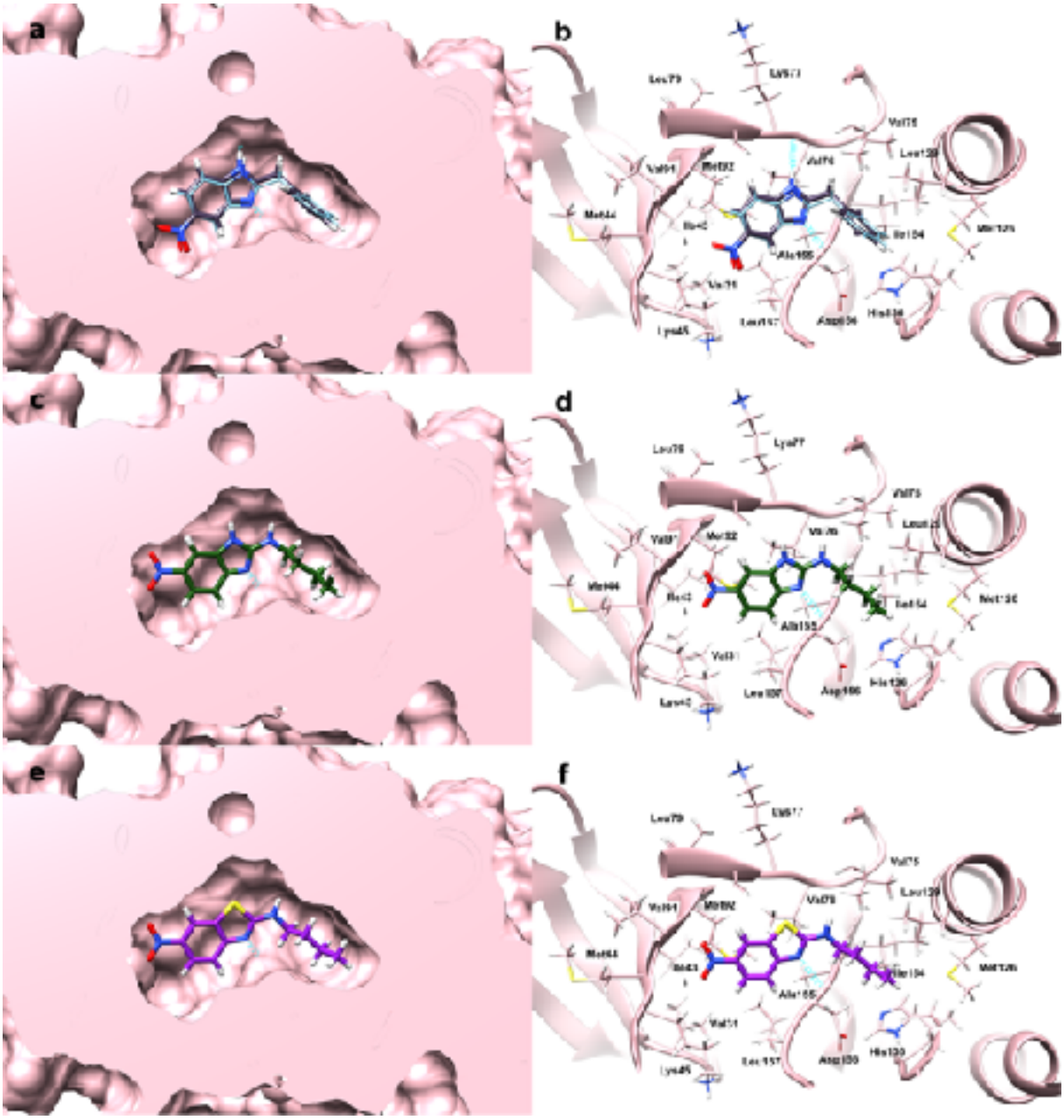

Figure 6. Docking conformations of selected RIPK1 inhibitors. (**a**, **b**) Docking conformation (brown) superposed on the X-ray structure (cyan, PDB code 6C3E) [14]of 2-benzyl-5-nitro-1*H*-benzimidazole in the binding site of RIPK1; (**c**, **d**) Docking conformation of **AV123 (12)** in the binding site of RIPK1; (**e**, **f**) Docking conformation of **MBM105** (**67**) in the binding site of RIPK1. The protein is represented as pink surface (**a**, **c**, **e**) or cartoon with

residues within 5 Å from the ligand visible (**b**, **d**, **f**). Hydrogen bonds are represented as cyan colored springs.

3. Conclusion

In this study, we identified the first marine-derived compounds as RIPK1 inhibitors that can block necroptotic cell death. This new series of derivatives are based on the 2-aminobenzazole scaffold, a building brick of the larger benzosceptrin C extracted from a marine sponge. Among the 54 compounds synthesized, the 2-aminobenzimidazole **AV123 (12)** and the 2-aminobenzothiazole **MBM105** (**67**) significantly blocked the necroptotic cell-death induced by TNF-α in human FADD-deficient Jurkat T cells with EC_{50} values in the low micromolar range (1.7 and 4.7 μM, respectively). We have shown also that the inhibition of the catalytic activity of RIPK1 can explain the cellular effect observed. In particular, hit compound **MBM105** (**67**) showed the best inhibitory effect against HsRIPK1, with an IC_{50} value of 2.89 μM. This compound is also rather selective toward a panel of 12 disease-related protein kinases. In vitro studies on human RPE1 retina cells and Jurkat wild-type lymphocyte cells confirmed their interest. Indeed, **MBM105** (**67**) is non-cytotoxic and blocks the necroptotic but not the apoptotic cell death. Thus, the 2-aminobenzothiazole **MBM105** (**67**) represents an attractive chemical probe for the study of necroptosis but also serves as a new chemical platform for further development of innovative therapeutic modalities.

4. Experimental part

4.1. Chemistry

4.1.1. General considerations

All reagents were of analytical grade and were used without further purification. All reactions were monitored by TLC using pre-coated silica gel aluminium plates (Macherey–Nagel) and visualized by UV light (254 nm). Flash column chromatography was carried out with silica gel 60 (70–230 mesh, Macherey–Nagel). ^{1}H and ^{13}C NMR spectra were acquired at 300 and 75 MHz, respectively, on Bruker spectrometers: Avance 300 MHz (QNP-^{13}C, ^{31}P, ^{19}F -probe or Dual ^{13}C probe) and Avance 500 MHz (BBO-ATM probe or BBI-ATM probe). Chemical

shifts (d) are reported in parts per million (ppm) relative to the residual solvent signals, and coupling constants (J) are reported in hertz (Hz). The following abbreviations are used: s, singlet; d, doublet; dd, doublet of doublet; t, triplet; q, quadruplet; quintuplet, quint; dhept, doublet of heptuplet; m, multiplet. IR spectra were recorded on a PerkinElmer Spectrum 65 spectrophotometer using an attenuated total reflectance (ATR) device (ν in cm-1). High-resolution MS data were obtained on a Waters LCT Micromass spectrometer in positive electrospray ionization-time of flight (ESI-TOF) mode. Reported yields are unoptimized.

4.1.2. General procedures for the synthesis of 2-Aminobenzimidazoles 12-49

Procedure A

A mixture of the corresponding substituted-phenylenediamine (limiting reagent), isothiocyanate (1.2 equiv.) and dialkylcarbodiimide (1.2 equiv.) was stirred in pyridine or acetonitrile (3 mL) at 80 °C for 16 h. After, the reaction mixture was evaporated to remove volatiles. The residue was either purified by flash column chromatography on silica gel (CH_2Cl_2/CH_3OH: 95/5) or filtrated and washed with a 1:1 mixture of Et_2O and acetonitrile (3x10 mL).

Procedure B

A mixture of the corresponding *o*-phenylenediamine (limiting reagent), isonitrile (1.5 equiv), 1 mol% elemental selenium powder and pyridine (0.2 mL) were added at rt. The mixture was then charged with oxygen (1 atm) and stirred at the appropriate temperature for 24 h. After the reaction time, the reaction was filtered to remove solid particles. The filtrate was dried to remove volatiles. The residue was purified by flash column chromatography on silica gel (CH_2Cl_2/CH_3OH : 95/5).

***N*-Butyl-6-nitro-1*H*-benzo[*d*]imidazol-2-amine AV123 (12)**

4-Nitro-*o*-phenylenediamine (459 mg, 3 mmol), *n*-butyl isothiocyanate (434 µL, 3.6 mmol), diisopropylcarbodiimide (561 µL, 3.6 mmol) were reacted in pyridine (1 mL) according to the procedure A for the synthesis of the 2-aminobenzimidazoles. Flash column chromatography afforded **AV123 (12)** (632 mg, 90%) as a yellow amorphous solid. IR (neat): 3279, 2955, 2937, 1650, 1470, 1320, 1254, 1064, 991 cm^{-1}. ^1H NMR (300 MHz, DMSO-*d6*) δ 11.27 (s, 1H), 7.93 (d, J = 2.2 Hz, 1H), 7.88 (d, J = 8.3 Hz, 1H), 7.45 (s, 1H), 7.20 (d, J = 8.7 Hz, 1H),

3.47 – 3.16 (m, 2H), 1.65 – 1.45 (m, 1H), 1.35 (dq, *J* = 14.1, 7.2 Hz, 1H), 0.90 (t, *J* = 7.3 Hz, 1H). ^{13}C NMR (75 MHz, DMSO-*d6*) δ 159.3, 150.8, 138.9, 133.2, 117.6, 113.1, 104.2, 41.8, 31.3, 19.5, 13.6. HRMS ESI-TOF [*M*+H]$^+$ *m/z* calcd for $C_{11}H_{15}N_4O_3$. 235.1195, Found: 235.1195.

_N_-Ethyl-6-nitro-1_H_-benzo[_d_]imidazol-2-amine (13)

4-Nitro-*o*-phenylenediamine (459 mg, 3 mmol), ethyl isothiocyanate (315 µL, 3.6 mmol), diisopropylcarbodiimide (557 µL, 3.6 mmol) were reacted in pyridine according to the procedure A for the synthesis of the 2-aminobenzimidazoles. Flash column chromatography afforded compound **13** (436 mg, 70%) as a light yellow foam. IR (neat): 3270, 2983, 1661, 1608, 1582, 1473, 1256, 1123, 1060, 1018 cm^{-1}. ^{1}H NMR (300 MHz, CD_3OD) δ 8.00 (d, *J* = 2.2 Hz, 1H), 7.94 (dd, *J* = 8.7, 2.2 Hz, 1H), 7.20 (d, *J* = 8.7 Hz, 1H), 3.42 (q, *J* = 7.1 Hz, 2H), 1.28 (t, *J* = 7.1 Hz, 3H). ^{13}C NMR (75 MHz, CD_3OD) δ 160.0, 146.7, 142.8, 134.3, 118.5, 112.4, 107.9, 38.9, 15.6. HRMS ESI-TOF [*M*+H]$^+$ *m/z* calcd for $C_9H_{11}N_4O_2$ 207.0882. Found 207.0873.

6-Nitro-_N_-propyl-1_H_-benzo[_d_]imidazol-2-amine (14)

4-Nitro-*o*-phenylenediamine (306 mg, 2 mmol), propyl isothiocyanate (250 µL, 2.4 mmol), diisopropylcarbodiimide (372 µL, 2.4 mmol) were reacted in acetonitrile according to the for the synthesis of the 2-aminobenzimidazoles. The resulting solid was filtrated and washed with a 8:2 mixture of Et_2O and acetonitrile (3x10 mL) to afford compound **14** (211 mg, 48%) as a yellow amorphous solid. IR (neat): 3330, 2959, 1659, 1581, 1471, 1446, 1255, 1220, 1061, 992, 883 cm^{-1}.^{1}H NMR (300 MHz, DMSO) δ 11.28 (s, 1H), 7.93 (d, *J* = 2.3 Hz, 1H), 7.87 (dd, *J* = 8.7, 2.3 Hz, 1H), 7.37 (s, 1H), 7.19 (d, *J* = 8.7 Hz, 1H), 3.28 (dd, *J* = 13.1, 6.7 Hz, 2H), 1.70 – 1.47 (m, 2H), 0.91 (t, *J* = 7.4 Hz, 3H).^{13}C NMR (75 MHz, DMSO-*d6*) δ 158.99, 116.93, 112.16, 105.17, 43.87, 22.45, 11.21. Some quaternary carbons and aromatic CH too broad to be seen due to very slow relaxation. HRMS ESI-TOF [*M*+H]$^+$ *m/z* calcd for $C_{10}H_{13}N_4O_2$ 221.1039. Found: 221.1037.

6-Nitro-_N_-hexyl-1_H_-benzo[_d_]imidazol-2-amine (15)

4-Nitro-*o*-phenylenediamine (459 mg, 3 mmol), *n*-hexyl isothiocyanate (591 µL, 3.6 mmol), diisopropylcarbodiimide (557 µL, 3.6 mmol) were reacted in pyridine according to the procedure A for the synthesis of the 2-aminobenzimidazoles. Flash column chromatography afforded compound **15** (584 mg, 74%) as a yellow amorphous solid. IR (neat): 3337, 3107, 2955, 2856, 1660, 1586, 1465, 1263, 1067, 944 cm^{-1}. ^{1}H NMR (300 MHz, DMSO-*d6*) δ 11.27 (s, 1H), 7.94 (d, J = 2.3 Hz, 1H), 7.87 (dd, J = 8.7, 2.3 Hz, 1H), 7.35 (s, 1H), 7.19 (d, J = 8.7 Hz, 1H), 3.31 (dd, J = 12.8, 6.8 Hz, 2H), 1.69 – 1.42 (m, 2H), 1.46 – 1.16 (m, 6H), 0.84 (t, J = 6.8 Hz, 3H). ^{13}C NMR (75 MHz, DMSO-*d6*) δ 158.94, 159.58, 116.85, 112.23, 104.91, 42.13, 30.96, 29.16, 25.98, 22.03, 13.81. Some quaternary carbons and aromatic CH too broad to be seen due to very slow relaxation. HRMS ESI-TOF $[M+H]^+$ *m/z* calcd for $C_{13}H_{19}N_4O_2$ 263.1508. Found: 263.1495.

6-Nitro-*N*-octyl-1*H*-benzo[*d*]imidazol-2-amine (16)

4-Nitro-*o*-phenylenediamine (459 mg, 3 mmol), *n*-octyl isothiocyanate (678 µL, 3.6 mmol), diisopropylcarbodiimide (557 µL, 3.6 mmol) were reacted in pyridine according to the procedure A for the synthesis of the 2-aminobenzimidazoles. Flash column chromatography afforded compound **16** (508 mg, 58%) as a yellow amorphous solid. IR (neat): 3348, 2923, 2853, 1660, 1586, 1466, 1269, 1067, 944 cm^{-1}. ^{1}H NMR (300 MHz, DMSO-*d6*) δ 11.27 (s, 1H), 7.93 (s, 1H), 7.87 (d, J = 8.6 Hz, 1H), 7.29 (m, 1H), 7.20 (d, J = 8.6 Hz, 1H), 1.76 – 1.41 (m, 2H), 1.41 – 1.08 (m, 12H), 0.94 – 0.68 (m, 3H). ^{13}C NMR (75 MHz, DMSO-*d6*) δ 158.94, 139.56, 116.76, 111.49, 105.48, 42.12, 31.18, 29.19, 28.68, 28.64, 26.31, 22.01, 13.84. Some quaternary carbons and aromatic CH too broad to be seen due to very slow relaxation. HRMS ESI-TOF $[M+H]^+$ *m/z* calcd for $C_{15}H_{22}N_4O_2$ 291.1821. Found: 291.1825.

***N*-Isopropyl-6-nitro-1*H*-benzo[*d*]imidazol-2-amine (17)** [26]

4-Nitro-*o*-phenylenediamine (459 mg, 3 mmol), isopropyl isothiocyanate (384 µL, 3.6 mmol), diisopropylcarbodiimide (557 µL, 3.6 mmol) were reacted in pyridine according to the procedure A for the synthesis of the 2-aminobenzimidazoles. Flash column chromatography afforded **17** (607 mg, 92%) as a light yellow amorphous solid. ^{1}H NMR (300 MHz, CD_3OD) δ 8.00 (d, J = 2.2 Hz, 1H), 7.94 (dd, J = 8.7, 2.2 Hz, 1H), 7.20 (d, J = 8.7 Hz, 1H), 3.98 (m,

1H), 1.29 (d, *J* = 6.6 Hz, 6H). ^{13}C NMR (75 MHz, CD_3OD) δ 159.3, 149.6, 142.9, 135.0, 118.4, 112.4, 107.9, 46.0, 23.3.

_N_-Allyl-6-nitro-1_H_-benzo[_d_]imidazol-2-amine (18)

4-Nitro-*o*-phenylenediamine (459 mg, 3 mmol), allyl isothiocyanate (352 µL, 3.6 mmol), diisopropylcarbodiimide (557 µL, 3.6 mmol) were reacted in pyridine according to the procedure A for the synthesis of the 2-aminobenzimidazoles. Flash column chromatography afforded compound **18** (522 mg, 80%) as a light yellow amorphous solid. IR (neat): 3280, 2976, 1665, 1606, 1583, 1475, 1319, 1256, 1219, 1062, 1004, 922, 880, 816 cm^{-1}. ^{1}H NMR (300 MHz, CD_3OD) δ 8.02 (d, *J* = 2.3 Hz, 1H), 7.96 (dd, *J* = 8.8, 2.3 Hz, 1H), 7.22 (d, *J* = 8.8 Hz, 1H), 5.99 (m, 1H), 5.29 (m, 1H), 5.16 (m, 1H), 4.02 (m, 2H). 2H missing due to chemical exchange with MeOD. ^{13}C NMR (75 MHz, DMSO-*d6*) δ 158.7, 139.7, 135.4, 116.9, 115.3, 112.6, 105.1, 44.3. Some quaternary carbons and aromatic CH too broad to be seen due to very slow relaxation. HRMS ESI-TOF $[M+H]^+$ *m/z* calcd for $C_{10}H_{11}N_4O_2$: 219.0867. Found 219.0882.

6-Nitro-_N_-(prop-2-yn-1-yl)-1_H_-benzo[_d_]imidazol-2-amine (19)

4-Nitro-*o*-phenylenediamine (306 mg, 2 mmol), propargyl isothiocyanate (226 µL, 2.4 mmol), diisopropylcarbodiimide (372 µL, 2.4 mmol) were reacted in acetonitrile according to the procedure A for the synthesis of the 2-aminobenzimidazoles. Flash column chromatography afforded compound **19** (133 mg, 26%) as a yellow amorphous solid. IR (neat): 3332, 3266, 2903, 2740, 2643, 1574, 1466, 1320, 1066, 1037, 867, 819 cm^{-1}. ^{1}H NMR (300 MHz, DMSO) δ 11.48 (s, 1H), 8.00 (s, 1H), 7.94 – 7.82 (m, 1H), 7.85 – 7.40 (m, 1H), 7.28 (d, *J* = 8.7 Hz, 1H), 4.16 (d, *J* = 3.2 Hz, 2H), 3.16 (s, 1H). ^{13}C NMR (75 MHz, DMSO-*d6*) δ 117.47, 115.46, 113.83, 109.91, 108.58, 104.75, 81.45, 73.38, 31.57. HRMS ESI-TOF $[M+H]^+$ *m/z* calcd. for $C_{10}H_9N_4O_2$ 217.0726. Found: 217.0718.

_N_-Isobutyl-6-nitro-1_H_-benzo[_d_]imidazol-2-amine (20)

4-Nitro-*o*-phenylenediamine (306 mg, 2 mmol), isobutyl isothiocyanate (291 µL, 2.4 mmol), diisopropylcarbodiimide (372 µL, 2.4 mmol) were reacted in acetonitrile according to the procedure A for the synthesis of the 2-aminobenzimidazoles. The resulting solid was filtrated

and washed with a 8:2 mixture of Et_2O and acetonitrile (3x10 mL) to afford compound **20** (114 mg, 24%) as a yellow amorphous solid. IR (neat): 3354, 3110, 2964, 1613, 1592, 1289, 1065, 1020, 816 cm^{-1}. ^1H NMR (300 MHz, DMSO-*d6*) δ 11.19 (s, 1H), 7.93 (d, J = 2.1 Hz, 1H), 7.87 (d, J = 8.7 Hz, 1H), 7.43 (s, 1H), 7.19 (d, J = 8.7 Hz, 1H), 3.14 (t, J = 6.4 Hz, 2H), 1.88 (dp, J = 13.4, 6.7 Hz, 1H), 0.91 (d, J = 6.7 Hz, 6H). ^{13}C NMR (75 MHz, DMSO-*d6*) δ 117.58, 113.00, 104.65, 49.63, 27.97, 22.66, 19.94. Some quaternary carbons and aromatic CH too broad to be seen due to very slow relaxation. HRMS ESI-TOF $[M+H]^+$ *m/z* calcd. for $C_{11}H_{15}N_4O_2$ 235.1195. Found: 235.1185.

***N*-(2-Methoxyethyl)-6-nitro-1*H*-benzo[*d*]imidazol-2-amine (21)**

4-Nitro-*o*-phenylenediamine (164 mg, 1.5 mmol), 2-methoxyethyl isothiocyanate (195 µL, 1.8 mmol), dicyclohexylcarbodiimide (371 mg, 1.8 mmol) were reacted in pyridine according to the procedure A for the synthesis of the 2-aminobenzimidazoles. Flash column chromatography afforded compound **21** (126 mg, 36%) as a light yellow solid. IR (neat): 3287, 2922, 2828, 1657, 1584, 1466, 1261, 1103, 1061 cm^{-1}. ^1H NMR (500 MHz, DMSO-*d6*) δ 11.21 (s, 1H), 7.94 (t, J = 9.1 Hz, 1H), 7.88 (dd, J = 8.7, 2.2 Hz, 1H), 7.43 (s, 1H), 7.22 (d, J = 8.7 Hz, 1H), 3.50 (m, 2H), 3.29 (s, 3H). ^{13}C NMR (75 MHz, DMSO-*d6*) δ 117.4, 113.3, 109.2, 104.5, 70.6, 58.0, 41.8. Some quaternary carbons and aromatic CH too broad to be seen due to very slow relaxation. HRMS ESI-TOF $[M+H]^+$ *m/z* calcd for $C_{10}H_{13}N_4O_2$ 237.0988. Found 237.0989.

***N*-Cyclohexyl-6-nitro-1*H*-benzo[*d*]imidazol-2-amine (22)** [27]

4-Nitro-*o*-phenylenediamine (229 mg, 1 mmol), cyclohexyl isocyanide (280 µL, 1.5 mmol), elemental selenium (1 mg, 1 mol%) and oxygen (1 atm) were reacted at 90°C in pyridine (0.2 mL) according to the procedure B for the synthesis of the 2-aminobenzimidazoles. Flash column chromatography afforded compound **22** (172 mg, 66%) as a pale yellow amorphous solid. ^1H NMR (300 MHz, CD_3OD) δ 8.02 (d, J = 7.9 Hz, 1H), 7.97 (d, J = 1.2 Hz, 1H), 7.22 (dd, J = 7.9, 1.2 Hz, 1H), 3.63 (m, 1H), 2.06-1.37 (m, 10H). ^{13}C NMR (75 MHz, CD_3OD) δ 150.6, 142.5, 139.0, 134.0, 117.7, 113.3, 104.2, 51.0, 32.7, 25.2, 24.6.

***N*-Benzyl-6-nitro-1*H*-benzo[*d*]imidazol-2-amine (23)** [26]

4-Nitro-*o*-phenylenediamine (459 mg, 3 mmol), phenyl isothiocyanate (430 µL, 3.6 mmol), diisopropylcarbodiimide (557 µL, 3.6 mmol) were reacted in pyridine according to the procedure A for the synthesis of the 2-aminobenzimidazoles. Flash column chromatography afforded compound **23** (624 mg, 78%) as a light yellow amorphous solid. ^{1}H NMR (300 MHz, DMSO-*d6*) δ 12.87 (s, 1H), 12.43 (s, 1H), 8.37 (d, J = 1.9 Hz, 1H), 8.18 – 7.94 (m, 3H), 7.75 – 7.46 (m, 4H). ^{13}C NMR (75 MHz, DMSO-*d6*) δ 166.7, 150.9, 141.9, 132.8, 132.5, 128.5, 128.3, 117.4.

***N*-(6-Nitro-1*H*-benzo[*d*]imidazol-2-yl)benzamide (24)** [27]

4-Nitro-*o*-phenylenediamine (459 mg, 3 mmol), benzyl isothiocyanate (477 µL, 3.6 mmol), diisopropylcarbodiimide (557 µL, 3.6 mmol) were reacted in pyridine according to procedure A for the synthesis of the 2-aminobenzimidazoles. Flash column chromatography afforded compound **25** (561 mg, 66%) as a light yellow amorphous solid. ^{1}H NMR (300 MHz, MeOD) δ 8.03 (d, J = 2.2 Hz, 1H), 8.00 – 7.88 (m, 1H), 7.46 – 7.29 (m, 4H), 7.29 – 7.13 (m, 2H), 4.61 (s, 2H), 2H missing due to chemical exchange with MeOD. ^{13}C NMR (75 MHz, MeOD) δ 140.0, 129.6, 128.3, 128.4, 118.3, 112.5, 107.8, 47.3. Some quaternary carbons and aromatic CH too broad to be seen due to very slow relaxation. HRMS ESI-TOF $[M+H]^+$ *m/z* calcd for $C_{14}H_{13}N_4O_2$ 269.1039. Found 269.1036.

6-Nitro-*N*-phenyl-1*H*-benzo[*d*]imidazol-2-amine (25)

4-Nitro-*o*-phenylenediamine (459 mg, 3 mmol), benzoyl isothiocyanate (484 µL, 3.6 mmol), diisopropylcarbodiimide (557 µL, 3.6 mmol) were reacted in pyridine according to the procedure A for the synthesis of the 2-aminobenzimidazoles. Flash column chromatography afforded compound **25** (528 mg, 70%) as a light yellow amorphous solid. IR (neat): 3287, 2975, 2868, 1642, 1577, 1455, 1318, 1256, 1061, 996 cm^{-1}. ^{1}H NMR (300 MHz, DMSO-*d6*) δ 11.44 (s, 1H), 9.94 (s, 1H), 8.15 (d, J = 2.3 Hz, 1H), 7.97 (dd, J = 8.7, 2.3 Hz, 1H), 7.75 (dd, J = 8.6, 1.0 Hz, 2H), 7.43 (d, J = 8.7 Hz, 1H), 7.38 – 7.25 (m, 2H), 7.00 (t, J = 7.4 Hz, 1H). ^{13}C NMR (75 MHz, DMSO-*d6*) δ 139.7, 128.9, 121.7, 117.9, 117.0. Some quaternary carbons and aromatic CH too broad to be seen due to very slow relaxation. HRMS ESI-TOF $[M+H]^+$ *m/z* calcd for $C_{14}H_{11}N_4O_3$ 283.0831. Found 283.0835.

_N_-(4-Bromophenyl)-6-nitro-1_H_-benzo[_d_]imidazol-2-amine (26)

4-Nitro-*o*-phenylenediamine (306 mg, 2 mmol), 4-bromophenyl isothiocyanate (513 mg, 2.4 mmol), diisopropylcarbodiimide (372 µL, 2.4 mmol) were reacted in acetonitrile according to the procedure A for the synthesis of the 2-aminobenzimidazoles. The resulting solid was filtrated and washed with a 8:2 mixture of Et_2O and acetonitrile (3x10 mL) to afford compound **26** (286 mg, 43%) as a yellow amorphous solid. IR (neat): 3279, 2845, 1661, 1572, 1491, 1315, 1273, 1072, 1010, 891 cm^{-1}. ^1H NMR (300 MHz, DMSO) δ 11.52 (s, 1H), 10.07 (s, 1H), 8.16 (d, J = 2.3 Hz, 1H), 7.98 (dd, J = 8.8, 2.3 Hz, 1H), 7.81 – 7.71 (m, 2H), 7.59 – 7.48 (m, 2H), 7.45 (d, J = 8.7 Hz, 1H). ^{13}C NMR (75 MHz, DMSO-*d6*) δ 153.73, 141.05, 139.20, 131.58, 119.74, 117.05, 112.99. Some quaternary carbons and aromatic CH too broad to be seen due to very slow relaxation. HRMS ESI-TOF $[M+H]^+$ *m/z* calcd for $C_{13}H_9{}^{79}BrN_4O_2$ 332.9987. Found: 332.9991.

4-((6-Nitro-1_H_-benzo[_d_]imidazol-2-yl)amino)benzonitrile (27)

4-Nitro-*o*-phenylenediamine (306 mg, 2 mmol), (218 mg, 2 mmol), 4-cyanophenyl isothiocyanate (384 mg, 2.4 mmol), diisopropylcarbodiimide (372 µL, 2.4 mmol) were reacted in acetonitrile according to the procedure A for the synthesis of the 2-aminobenzimidazoles. The resulting solid was filtrated and washed with a 8:2 mixture of Et_2O and acetonitrile (3x10 mL) to afford compound **27** (488 mg, 87%) as a yellow amorphous solid. IR (neat): 3274, 2842, 2226, 1658, 1562, 1505, 1320, 1233, 1178, 1066, 1020 cm^{-1}. ^1H NMR (300 MHz, DMSO-*d6*) δ 11.68 (s, 1H), 10.50 (s, 1H), 8.23 (d, J = 2.2 Hz, 1H), 8.07 – 7.89 (m, 3H), 7.89 – 7.71 (m, 2H), 7.52 (d, J = 8.8 Hz, 1H). ^{13}C NMR (75 MHz, DMSO) δ 144.0, 133.4, 119.4, 117.6, 102.8. Some quaternary carbons and aromatic CH too broad to be seen due to very slow relaxation. HRMS ESI-TOF $[M+H]^+$ *m/z* calcd for $C_{14}H_{10}N_5O_2$ 280.0834. Found: 280.0840.

6-Nitro-N-(4-(trifluoromethyl)phenyl)-1H-benzo[d]imidazol-2-amine (28)

4-Nitro-*o*-phenylenediamine (306 mg, 2 mmol), (218 mg, 2 mmol), 4-(trifluoromethyl)-phenyl isothiocyanate (487 mg, 2.4 mmol), diisopropylcarbodiimide (372 µL, 2.4 mmol) were reacted in acetonitrile according to the procedure A for the synthesis of the 2-aminobenzimidazoles. The resulting solid was filtrated and washed with a 8:2 mixture of Et_2O and acetonitrile (3x10 mL) to afford compound **28** (224 mg, 35%) as a yellow amorphous

solid. IR (neat): 3317, 1615, 1572, 1320, 1284, 1098, 1066, 1015, 822 cm^{-1}. ^{1}H NMR (300 MHz, DMSO-*d6*) δ 11.64 (s, 1H), 10.37 (s, 1H), 8.21 (d, J = 2.2 Hz, 1H), 8.07 – 7.91 (m, 3H), 7.70 (d, J = 8.6 Hz, 2H), 7.50 (d, J = 8.8 Hz, 1H). ^{13}C NMR (75 MHz, DMSO-*d6*) δ 153.25, 143.35, 141.19, 116.19, 121.40 (q, J = 40 Hz, 1C), 117.43, 117.12. Some quaternary carbons and aromatic CH too broad to be seen due to very slow relaxation. ^{19}F NMR (282 MHz, DMSO-*d6)* δ – 59.96 (s, 3F). HRMS ESI-TOF $[M+H]^+$ *m/z* calcd for $C_{14}H_{10}F_3N_4O_2Na$ 364.0997. Found: 364.0998.

6-Nitro-*N*-(4-nitrophenyl)-1*H*-benzo[*d*]imidazol-2-amine (29)

4-Nitro-*o*-phenylenediamine (306 mg, 2 mmol), (218 mg, 2 mmol), 4-nitrophenyl isothiocyanate (487 mg, 2.4 mmol), diisopropylcarbodiimide (372 µL, 2.4 mmol) were reacted in acetonitrile according to the procedure A for the synthesis of the 2-aminobenzimidazoles. The resulting solid was filtrated and washed with a 8:2 mixture of Et_2O and acetonitrile (3x10 mL) to afford compound **29** (488 mg, 87%) as a yellow solid. IR (neat): 3389, 3305, 3108, 2919, 1578, 1485, 1321, 1290, 1251, 1114, 1072 cm^{-1}. ^{1}H NMR (300 MHz, DMSO-*d6*) δ 11.42 (s, 1H), 8.24 (d, J = 8.9 Hz, 3H), 8.10 – 7.85 (m, 4H), 7.52 (d, J = 8.8 Hz, 1H). ^{13}C NMR (75 MHz, DMSO-*d6*) δ 153.01, 146.36, 143.02, 141.30, 140.48, 137.00, 125.24, 117.09, 116.91, 113.12, 108.68. HRMS ESI-TOF $[M+H]^+$ *m/z* calcd for $C_{13}H_{10}N_5O_4$ 300.0733. Found: 300.0737.

***N*^{1}, *N*^{1}-Dimethyl-*N*^{4}-(6-nitro-1*H*-benzo[*d*]imidazol-2-yl)benzene-1,4-diamine (30)**

4-Nitro-*o*-phenylenediamine (306 mg, 2 mmol), 4-dimethylaminophenyl isothiocyanate (427mg, 2.4 mmol), diisopropylcarbodiimide (372 µL, 2.4 mmol) were reacted in acetonitrile according to the procedure A for the synthesis of the 2-aminobenzimidazoles. The resulting solid was filtrated and washed with a 8:2 mixture of Et_2O and acetonitrile (3x10 mL) to afford compound **30** (416 mg, 70%) as a red amorphous solid. IR (neat): 3408, 2796, 1669, 1572, 1490, 1472, 1310, 1258, 1225, 1070, 945, 812 cm^{-1}. ^{1}H NMR (300 MHz, DMSO) δ 11.25 (s, 1H), 9.58 (s, 1H), 8.05 (d, J = 2.2 Hz, 1H), 7.93 (d, J = 8.1 Hz, 1H), 7.48 (d, J = 8.7 Hz, 2H), 7.33 (d, J = 8.7 Hz, 1H), 6.78 (d, J = 8.9 Hz, 2H), 2.87 (s, 6H). ^{13}C NMR (75 MHz, DMSO-*d6*) δ 146.78, 129.18, 120.68, 117.55, 113.24, 104.84, 40.61. Some quaternary carbons and

aromatic CH too broad to be seen due to very slow relaxation. HRMS ESI-TOF [*M*+H]$^+$ *m/z* calcd for $C_{15}H_{16}N_5O_4$ 298.1304. Found: 298.1306.

Ethyl (6-nitro-1H-benzo[d]imidazol-2-yl)glycinate (31)

4-Nitro-*o*-phenylenediamine (613 g, 4 mmol), Ethyl isothiocyanatoacetate (601 µL, 4.8 mmol), diisopropylcarbodiimide (743 µL, 4.8 mmol) were reacted in acetonitrile according to the procedure A for the synthesis of the 2-aminobenzimidazoles. Flash column chromatography afforded compound **31** (523 g, 49%) as a brown amorphous solid. **^{1}H NMR (300 MHz, MeOD)** δ 8.07 (d, J = 2.2 Hz, 1H), 7.99 (dd, J = 8.7, 2.2 Hz, 1H), 7.27 (d, J = 8.7 Hz, 1H), 4.23 (q, J = 7.1 Hz, 2H), 4.20 (s, 2H), 1.29 (t, J = 7.1 Hz, 3H). **^{13}C NMR (75 MHz, MeOD)** δ 118.4, 62.4, 44.9, 14.4. Some quaternary carbons are not visible.

6-Bromo-*N*-ethyl-1*H*-benzo[*d*]imidazol-2-amine (32)

4-Bromo-*o*-phenylenediamine (561 mg, 3 mmol), ethyl isothiocyanate (315 µL, 3.6 mmol), diisopropylcarbodiimide (557 µL, 3.6 mmol) were reacted in pyridine according to the procedure A for the synthesis of the 2-aminobenzimidazoles. Flash column chromatography afforded compound **32** (284 mg, 39%) as a deep red amorphous solid. ^{1}H NMR (300 MHz, $CDCl_3$) δ 7.36 (t, J = 9.1 Hz, 1H), 7.22 – 7.04 (m, 2H), 6.89 (s, 1H), 5.48 (s, 1H), 3.42 (q, J = 7.2 Hz, 2H), 1.21 (t, J = 7.2 Hz, 3H).^{13}C NMR (75 MHz, $CDCl_3$) δ 155.2, 138.9, 135.8, 123.8, 115.2, 113.6, 112.9, 38.1, 15.0. Some quaternary carbons and aromatic CH too broad to be seen due to very slow relaxation. HRMS ESI-TOF [*M*+H]$^+$ *m/z* calcd for $C_9H_{11}{}^{79}BrN_3$: 240.0136, found: 240.0146.

6-Bromo-*N*-butyl-1*H*-benzo[*d*]imidazol-2-amine (33)

4-Bromo-*o*-phenylenediamine (2 g, 10.7 mmol), *n*-butyl isothiocyanate (1.5 mL, 12.8 mmol), diisopropylcarbodiimide (2 mL, 12.8 mmol) were reacted in acetonitrile according to the procedure A for the synthesis of the 2-aminobenzimidazoles. Flash column chromatography afforded compound **33** (1.33 g, 46%) as a deep red hygroscopic solid. ^{1}H NMR (300 MHz, $CDCl_3$) δ 9.26 (s, 1H), 7.40 (d, J = 1.2 Hz, 1H), 7.14 (m, 2H), 5.38 (s, 1H), 3.41 (t, J = 7.1 Hz, 2H), 1.70 – 1.41 (m, 2H), 1.39 – 1.22 (q, J = 7.3 Hz, 2H), 0.85 (t, J = 7.3 Hz, 3H).^{13}C

NMR (75 MHz, $CDCl_3$) δ 156.4, 139.7, 136.5, 123.4, 115.1, 113.2, 112.8, 43.1, 31.9, 20.0, 13.7. HRMS ESI-TOF $[M+H]^+$ *m/z* calcd for $C_{11}H_{15}{}^{79}BrN_4$: 268.0449, found: 268.0444.

Methyl 2-(butylamino)-1*H*-benzo[d]imidazole-6-carboxylate (34)

Methyl 3,4-diaminobenzoate (664 g, 4 mmol), *n*-butyl isothiocyanate (435 µL, 4.8 mmol), diisopropylcarbodiimide (743 µL, 4.8 mmol) were reacted in acetonitrile according to the procedure A for the synthesis of the 2-aminobenzimidazoles. Flash column chromatography afforded compound **34** (813 mg, 82%) as a white amorphous solid. IR (neat): 3332, 3102, 2938, 1685, 1653, 1567, 1432, 1276, 1205, 1131, 1099, 999 cm^{-1}. ^1H NMR (300 MHz, DMSO-*d6*) δ 10.98 (s, 1H), 7.70 (d, J = 1.6 Hz, 1H), 7.58 (dd, J = 8.2, 1.6 Hz, 1H), 7.15 (d, J = 8.2 Hz, 1H), 6.97 (s, 1H), 3.80 (s, 3H), 3.27 (q, J = 7.3 Hz, 2H), 1.63 – 1.43 (m, 2H), 1.36 (dq, J = 14.2, 7.2 Hz, 2H), 0.91 (t, J = 7.3 Hz, 3H). ^{13}C NMR (75 MHz, DMSO-*d6*) δ 167.1, 157.5, 121.7, 112.1, 51.5, 31.4, 19.5, 13.7. Some quaternary carbons and aromatic CH too broad to be seen due to very slow relaxation. HRMS ESI-TOF $[M+H]^+$ *m/z* calcd for $C_{13}H_{18}N_3O_2$: 248.1399, found: 248.1398.

Ethyl 2-(butylamino)-1*H*-benzo[d]imidazole-7-carboxylate (35)

Ethyl 2,3-diaminobenzoate (665 g, 4 mmol), *n*-butyl isothiocyanate (435 µL, 4.8 mmol), diisopropylcarbodiimide (743 µL, 4.8 mmol) were reacted in acetonitrile according to the procedure A for the synthesis of the 2-aminobenzimidazoles. Flash column chromatography afforded compound **35** (820 g, 83%) as a brown amorphous solid. IR (neat): 3336, 2956, 1701, 1578, 1436, 1258, 1199, 1147, 1055, 1034 cm^{-1}. ^1H NMR (300 MHz, $CDCl_3$) δ 9.43 (s, 1H), 7.63 – 7.50 (m, 2H), 7.14 – 6.99 (m, 1H), 5.83 (s, 1H), 3.84 (s, 3H), 3.46 (t, J = 7.1 Hz, 2H), 1.66 – 1.49 (m, 2H), 1.43 – 1.27 (m, 2H), 0.87 (t, J = 7.3 Hz, 3H). ^{13}C NMR (75 MHz, $CDCl_3$) δ 167.5, 156.2, 144.0, 134.5, 120.6, 120.0, 111.0, 51.8, 42.8, 31.9, 23.4, 20.0, 13.7. HRMS ESI-TOF $[M+H]^+$ *m/z* calcd. for $C_{13}H_{18}N_3O_2$ 248.1399. Found: 248.1393.

Methyl 2-(cyclohexylamino)-1*H*-benzo[*d*]imidazole-6-carboxylate (36) [28]

Methyl 3,4-diaminobenzoate (249 mg, 1 mmol), cyclohexyl isocyanide (280 µL, 1.5 mmol), elemental selenium (1 mg, 1 mol%) and oxygen (1 atm) were reacted at 90°C in pyridine (0.2 mL) according to the procedure B for the synthesis of the 2-aminobenzimidazoles. Flash

column chromatography afforded compound **36** (154 mg, 56%) as a white amorphous solid. ^{1}H NMR (300 MHz, CD_3OD) δ 7.82 (d, J = 1.4 Hz, 1H), 7.71 (dd, J = 8.2, 1.4 Hz, 1H), 7.19 (d, J = 8.2 Hz, 1H), 3.87 (s, 3H, H16), 3.61 (m, 1H, H11), 2.06-1.35 (m, 10H). ^{13}C NMR (75 MHz, CD_3OD) δ 169.9, 145.2, 142.1, 134.7, 128.7, 124.0, 117.5, 113.1, 52.8, 52.4, 34.6, 26.9, 26.3.

***N*-isopropyl-7-nitro-1*H*-benzo[*d*]imidazol-2-amine (37)**

3-Nitro-*o*-phenylenediamine (459 mg, 3 mmol), phenyl isothiocyanate (384 µL, 3.6 mmol), diisopropylcarbodiimide (557 µL, 3.6 mmol) were reacted in pyridine according to the procedure A for the synthesis of the 2-aminobenzimidazoles. Flash column chromatography afforded compound **37** (630 mg, 95%) as a yellow solid. IR (neat): 3227, 3042, 2973, 1605, 1580, 1507, 1256, 1172, 1127, 1059 cm^{-1}. ^{1}H NMR (300 MHz, DMSO-*d6*) δ 11.29 (s, 1H), 7.67 (d, J = 8.4 Hz, 1H), 7.55 (d, J = 7.6 Hz, 1H), 7.09 (t, J = 8.1 Hz, 1H), 6.27 (d, J = 7.6 Hz, 1H), 3.98 (m, 1H), 1.23 (d, J = 6.5 Hz, 6H). ^{13}C NMR (75 MHz, DMSO-*d6*) δ 156.34, 147.23, 130.48, 128.74, 121.12, 119.95, 113.45, 43.96, 22.62. HRMS ESI-TOF [M+H]$^{+}$ *m/z* calcd. for $C_{10}H_{13}N_4O_2$ 221.1039 . Found: 221.1034.

***N*-Butyl-7-nitro-1*H*-benzo[*d*]imidazol-2-amine (38)**

3-Nitro-*o*-phenylenediamine (459 mg, 3 mmol), *n*-butyl isothiocyanate (434 µL, 3.6 mmol), diisopropylcarbodiimide (557 µL, 3.6 mmol) were reacted in pyridine according to the procedure A for the synthesis of the 2-aminobenzimidazoles. Flash column chromatography afforded compound **38** (665 mg, 95%) as a yellow amorphous solid. IR (neat): 3385, 2960, 2928, 1608, 1582, 1503, 1335, 1261, 1181 cm^{-1}. ^{1}H NMR (300 MHz, DMSO-*d6*) δ 11.47 (s, 1H), 7.68 (d, J = 8.2 Hz, 1H), 7.55 (d, J = 7.4 Hz, 1H), 7.09 (t, J = 7.8 Hz, 1H), 6.41 (s, 1H), 3.54 – 3.23 (m, 2H), 1.56 (dd, J = 14.0, 6.9 Hz, 2H), 1.36 (dd, J = 14.4, 7.2 Hz, 2H), 0.92 (t, J = 7.2 Hz, 3H). ^{13}C NMR (75 MHz, DMSO-*d6*) δ 157.72, 147.68, 130.94, 129.44, 121.53, 120.44, 113.90, 42.20, 31.78, 19.95, 14.14. HRMS ESI-TOF [M+H]$^{+}$ *m/z* calcd. for $C_{11}H_{15}N_4O_2$ 235.1195. Found: 235.1193.

***N*-(2-Methoxyethyl)-7-nitro-1*H*-benzo[*d*]imidazol-2-amine (39)**

3-Nitro-*o*-phenylenediamine (459 mg, 3 mmol), 2-methoxyethyl isothiocyanate (391 µL, 3.6 mmol), diisopropylcarbodiimide (557 µL, 3.6 mmol) were reacted in pyridine according to the procedure A for the synthesis of the 2-aminobenzimidazoles. Flash column chromatography afforded compound **39** (590 mg, 84%) as a red-orange amorphous solid. IR (neat): 3266, 2916, 2831, 1666, 1498, 1333, 1270, 1190, 1103 cm^{-1}. ^{1}H NMR (300 MHz, DMSO-*d6*) δ 11.51 (s, 1H), 7.66 (t, J = 14.1 Hz, 1H), 7.55 (d, J = 7.6 Hz, 1H), 7.10 (t, J = 8.0 Hz, 1H), 6.52 (s, 1H), 3.60 – 3.44 (m, 4H), 3.30 (s, 3H). ^{13}C NMR (75 MHz, DMSO-*d6*) δ 157.08, 146.96, 130.52, 128.86, 121.19, 120.00, 113.57, 70.56, 57.97. HRMS ESI-TOF $[M+H]^+$ *m/z* calcd. for $C_{10}H_{13}N_4O_3$ 237.0988. Found: 237.0983.

_N_-Butyl-7-nitro-1_H_-benzo[_d_]imidazol-2-amine (40)

3-Nitro-*o*-phenylenediamine (459 mg, 3 mmol), cyclohexyl isothiocyanate (510 µL, 3.6 mmol), diisopropylcarbodiimide (557 µL, 3.6 mmol) were reacted in pyridine according to the procedure A for the synthesis of the 2-aminobenzimidazoles. Flash column chromatography afforded compound **40** (394 mg, 50%) as a yellow amorphous solid. IR (neat): 3287, 2932, 2850, 1649, 1581, 1512, 1339, 1259, 1173, 1109, 1062 cm^{-1}.^{1}H NMR (300 MHz, DMSO-*d6*) δ 11.27 (s, 1H), 7.67 (d, J = 8.4 Hz, 1H), 7.55 (d, J = 7.6 Hz, 1H), 7.09 (t, J = 8.1 Hz, 1H), 6.38 (d, J = 7.9 Hz, 1H), 3.69 (s, 1H), 1.97 (d, J = 9.8 Hz, 2H), 1.82 – 1.62 (m, 2H), 1.47 – 1.15 (m, 6H). ^{13}C NMR (75 MHz, DMSO-*d6*) δ 156.27, 147.19, 130.42, 128.75, 121.05, 119.98, 113.40, 50.50, 32.43, 25.14, 24.13. HRMS ESI-TOF $[M+H]^+$ *m/z* calcd. for $C_{13}H_{17}N_4O_2$ 261.1352. Found: 261.1357.

7-Nitro-_N_-phenyl-1_H_-benzo[_d_]imidazol-2-amine (41)

3-Nitro-*o*-phenylenediamine (459 mg, 3 mmol), phenyl isothiocyanate (430 µL, 3.6 mmol), diisopropylcarbodiimide (557 µL, 3.6 mmol) were reacted in pyridine according to the procedure A for the synthesis of the 2-aminobenzimidazoles. Flash column chromatography afforded compound **41 AV118** (730 mg, 96%) as an orange-red amorphous solid. IR (neat): 3434, 3371, 3082, 1648, 1570, 1335, 1232, 1148, 1051, 987 cm^{-1}. ^{1}H NMR (300 MHz, DMSO-*d6*) δ 11.60 (s, 1H), 9.15 (s, 1H), 7.87 – 7.66 (m, 4H), 7.46 – 7.29 (m, 2H), 7.27 – 7.11 (m, 1H), 7.01 (t, J = 7.3 Hz, 1H).^{13}C NMR (75 MHz, DMSO-*d6*) δ 152.4, 146.4, 139.3,

131.0, 129.0, 127.5, 122.8, 121.6, 120.5, 117.2, 115.2. HRMS ESI-TOF $[M+H]^+$ *m/z* calcd. for $C_{13}H_{11}N_4O_2$ 255.0882. Found: 255.0880.

_N_-Benzyl-7-nitro-1_H_-benzo[_d_]imidazol-2-amine (42)

3-Nitro-*o*-phenylenediamine (459 mg, 3 mmol), benzyl isothiocyanate (477 µL, 3.6 mmol), diisopropylcarbodiimide (557 µL, 3.6 mmol) were reacted in pyridine according to the procedure A for the synthesis of the 2-aminobenzimidazoles. Flash column chromatography afforded compound **42** (586 mg, 73%) as an orange-red amorphous solid. IR (neat): 3375, 3074, 2964, 2869, 1656, 1584, 1495, 1332, 1274, 1221, 1113, 982, 910 cm^{-1}. ^1H NMR (300 MHz, DMSO-*d6*) δ 11.66 (s, 1H), 7.70 (d, J = 8.4 Hz, 1H), 7.55 (d, J = 7.3 Hz, 1H), 7.41 – 7.30 (m, 4H), 7.25 (ddd, J = 6.9, 3.8, 1.5 Hz, 1H), 7.10 (t, J = 7.8 Hz, 1H), 6.96 – 6.80 (m, 1H), 4.62 (d, J = 6.2 Hz, 2H). ^{13}C NMR (75 MHz, DMSO-*d6*) δ 157.18, 146.93, 139.56, 130.62, 128.94, 128.32, 127.05, 126.88, 121.30, 120.04, 113.68, 45.47. HRMS ESI-TOF $[M+H]^+$ *m/z* calcd. for $C_{14}H_{13}N_4O_2$ 269.1039. Found: 269.1038.

_N_-Cyclohexyl-6-methyl-1_H_-benzo[_d_]imidazol-2-amine (43) [29]

4-Methyl-*o*-phenylenediamine (183 mg, 1 mmol), cyclohexyl isocyanide (280 µL, 1.5 mmol), elemental selenium (1 mg, 1 mol%) and oxygen (1 atm) were reacted at 90°C in pyridine (0.2 mL) according to the procedure B for the synthesis of the 2-aminobenzimidazoles. Flash column chromatography afforded compound **43** (170 mg, 74%) as a brown amorphous solid. ^1H NMR (300 MHz, CD_3OD) δ 7.03 (d, J = 7.9 Hz, 1H), 6.98 (d, J = 1.2 Hz, 1H), 6.75 (dd, J = 7.9, 1.2 Hz, 1H), 3.55 (m, 1H), 2.32 (s, 3H), 2.01-1.30 (m, 10H).^{13}C NMR (75 MHz, CD_3OD) δ 156.2, 139.3, 137.0, 130.8, 122.2, 113.1, 112.3, 52.8, 34.7, 26.9, 26.2, 21.8.

6-Chloro-_N_-cyclohexyl-1_H_-benzo[_d_]imidazol-2-amine (44) [30]

4-Chloro-*o*-phenylenediamine (214 mg, 1 mmol), cyclohexyl isocyanide (280 µL, 1.5 mmol), elemental selenium (1 mg, 1 mol%) and oxygen (1 atm) were reacted at 90°C in pyridine (0.2 mL) according to the procedure B for the synthesis of the 2-aminobenzimidazoles. Flash column chromatography afforded compound **44** (204 mg, 82%) as a pale yellow solid. ^1H NMR (300 MHz, CD_3OD) δ 7.14 (d, J = 2.0 Hz, 1H), 7.08 (d, J = 8.3 Hz, 1H), 6.90 (dd, J =

8.3, 2.0 Hz, 1H), 3.57 (s, 1H), 2.05-1.36 (m, 10H).^{13}C NMR (75 MHz, CD_3OD) δ 157.2, 143.7, 140.8, 126.6, 121.0, 113.1, 112.9, 52.9, 34.7, 26.9, 26.3.

6-Bromo-*N*-cyclohexyl-1*H*-benzo[*d*]imidazol-2-amine (45)

4-Bromo-*o*-phenylenediamine (214 mg, 1 mmol), cyclohexyl isocyanide (280 µL, 1.5 mmol), elemental selenium (1 mg, 1 mol%) and oxygen (1 atm) were reacted at 100°C in pyridine (0.2 mL) according to the procedure B for the synthesis of the 2-aminobenzimidazoles. Flash column chromatography afforded compound **45** (206 mg, 70%) as a black oil. IR (neat): 2971, 2901, 1632, 1572, 1463, 1394, 1259, 1066, 1048, 879, 798 cm^{-1}.^{1}H NMR (300 MHz, CD_3OD) δ 7.23 (d, J = 1.9 Hz, 1H), 7.04 (d, J = 8.3 Hz, 1H), 6.95 (dd, J = 8.3, 1.9 Hz, 1H), 6.69 (d, J = 8.0 Hz, 1H), 3.54 (m, 1H), 1.93-1.25 (m, 10H).^{13}C NMR (75 MHz, CD_3OD) δ 155.6, 143.9, 135.5, 121.0, 115.8, 114.6, 113.4, 50.9, 32.9, 25.3, 24.7.HRMS ESI-TOF [M+H]$^+$ *m/z* calcd for $C_{13}H_{17}BrN_3$ 294.0606. Found 294.0602.

***N*-Butyl-6-iodo-1*H*-benzo[*d*]imidazol-2-amine (46)**

4-Iodo-*o*-phenylenediamine (306 mg, 2 mmol), (218 mg, 2 mmol), *n*-butyl isothiocyanate (289 µL, 2.4 mmol), diisopropylcarbodiimide (372 µL, 2.4 mmol) were reacted in acetonitrile according to the procedure A for the synthesis of the 2-aminobenzimidazoles. The resulting solid was filtrated and washed with a 8:2 mixture of Et_2O and acetonitrile (3x10 mL) to afford compound **46** (273 mg, 43%) as a brown foam. **IR (neat):** 3395, 2955, 2927, 1629, 1594, 1568, 1458, 1264, 1014, 902 cm^{-1}. ^{1}H NMR (300 MHz, DMSO-*d6*) δ 10.84 (s, 1H), 7.43 (d, J = 1.5 Hz, 1H), 7.14 (dd, J = 8.1, 1.6 Hz, 1H), 6.96 (d, J = 8.1 Hz, 1H), 6.85 – 6.67 (m, 1H), 3.28 (q, J = 6.7 Hz, 2H), 1.64 – 1.45 (m, 2H), 1.45 – 1.24 (m, 2H), 0.90 (t, J = 7.0 Hz, 3H). ^{13}C NMR (75 MHz, DMSO-*d6*) δ 156.07, 127.03, 119.90, 113.35, 81.48, 41.88, 31.45, 19.55, 13.71. Some quaternary carbons and aromatic CH too broad to be seen due to very slow relaxation. HRMS ESI-TOF [M+H]$^+$ *m/z* calcd. for $C_{11}H_{14}{}^{127}IN_3$ 316.0311. Found: 316.0326.

***N*-Butyl-6-(1*H*-tetrazol-1-yl)-1*H*-benzo[*d*]imidazol-2-amine (47)**

4-(1*H*-Tetrazol-1-yl)benzene-1,2-diamine (352mg, 2 mmol), *n*-butyl isothiocyanate (288 µL, 2.4 mmol), diisopropylcarbodiimide (372 µL, 2.4 mmol) were reacted in acetonitrile according to the procedure A for the synthesis of the 2-aminobenzimidazoles. The resulting

solid was filtrated and washed with a 8:2 mixture of Et_2O and acetonitrile (3x10 mL) to afford compound **47** (250 mg, 48%) as a beige foam. **IR (neat):** 2958, 2930, 1678, 1586, 1462, 1404, 1276, 1090, 1002, 918 cm^{-1}. ^1H NMR (300 MHz, DMSO) δ 11.17 (s, 1H), 9.94 (s, 1H), 7.57 (d, J = 1.8 Hz, 1H), 7.40 – 7.20 (m, 2H), 6.94 (t, J = 5.6 Hz, 1H), 3.30 (dd, J = 12.8, 6.9 Hz, 2H), 1.66 – 1.44 (m, 2H), 1.36 (dq, J = 14.2, 7.2 Hz, 2H), 0.96 – 0.81 (m, 3H). ^{13}C NMR (75 MHz, DMSO-*d6*) δ 171.92, 157.30, 142.14, 139.52, 126.12, 112.47, 111.14, 105.13, 41.86, 31.39, 19.52, 13.67. HRMS ESI-TOF $[M+H]^+$ *m/z* calcd for $C_{12}H_{16}N_7$ 258.1467. Found: 258.1463.

2-(Butylamino)-1*H*-benzo[*d*]imidazole-6-carbonitrile (48)

4-Cyano-*o*-phenylenediamine (266 mg, 2 mmol), *n*-butyl isothiocyanate (289 µL, 2.4 mmol), diisopropylcarbodiimide (372 µL, 2.4 mmol) were reacted in acetonitrile according to the procedure A for the synthesis of the 2-aminobenzimidazoles. Flash column chromatography afforded compound **48** (58 mg, 14%) as a white amorphous solid. IR (neat): 3267, 2949, 2867, 2213, 1663, 1605, 1568, 1287, 1126, 997 cm^{-1}. ^1H NMR (300 MHz, DMSO) δ 11.16 (s, 1H), 7.46 (s, 1H), 7.32 – 7.12 (m, 2H), 7.06 (s, 1H), 3.39 – 3.14 (m, 2H), 1.66 – 1.44 (m, 2H), 1.44 – 1.24 (m, 2H), 0.88 (t, J = 7.2 Hz, 3H). ^{13}C NMR (75 MHz, DMSO-*d6*) δ 157.62, 123.88, 120.87, 113.32, 41.79, 31.34, 19.49, 13.65. Some quaternary carbons and aromatic CH too broad to be seen due to very slow relaxation. HRMS ESI-TOF $[M+H]^+$ *m/z* calcd. for $C_{12}H_{15}N_4$ 215.1297. Found: 215.1301.

7-Bromo-*N*-butyl-5-(trifluoromethyl)-1H-benzo[*d*]imidazol-2-amine (49)

3-Bromo-5-(trifluoromethyl)benzene-1,2-diamine (510 mg, 2 mmol), *n*-butyl isothiocyanate (289 µL, 2.4 mmol), diisopropylcarbodiimide (372 µL, 2.4 mmol) were reacted in acetonitrile according to the procedure A for the synthesis of the 2-aminobenzimidazoles. Flash column chromatography afforded compound **49** (264 mg, 39%) as a white amorphous solid. IR (neat): 3413, 2933, 1641, 1598, 1425, 1313, 1111, 963 cm^{-1}. ^1H NMR (300 MHz, DMSO-*d6*) δ 11.34 (s, 1H), 7.38 (m, 3H), 3.32 (dd, J = 12.9, 6.8 Hz, 2H), 1.67 – 1.47 (m, 2H), 1.43 – 1.25 (m, 2H), 0.89 (t, J = 7.3 Hz, 3H). ^{13}C NMR (75 MHz, DMSO-*d6*) δ 157.73, 145.50, 133.96, 126.35, 122.76, 119.65, 106.28, 104.71, 41.83, 31.40, 19.44, 13.58.^{19}F NMR (282 MHz,

DMSO-*d6)* δ – 58.53 (s, 3F). HRMS ESI-TOF [*M*+H]$^+$ *m/z* calcd for $C_{12}H_{14}{}^{79}BrF_3N_3$ 336.0323. Found: 336.0326.

4.1.3. General procedures for the Suzuki-Miyaura cross-coupling reaction

A mixture of aryl bromide (1 equiv.), boronic acid (1 equiv.) and base (3 equiv.) in dioxanne (1mL) and water (0.1 mL) was degassed under a flow of Argon for 5 minutes. Palladium catalyst (5 mol%) was then added and the reaction mixture was heated at 80°C for 16h. The reaction mixture was allowed to cool to room temperature then concentrated under reduced pressure. The crude was purified by flash column chromatography on silica gel (CH_2Cl_2/ CH_3OH: 95/5).

6-(2-Chlorophenyl)-*N*-ethyl-1*H*-benzo[*d*]imidazol-2-amine (50)

6-Bromo-*N*-ethyl-1*H*-benzo[*d*]imidazol-2-amine (108 mg, 0.45 mmol), (2-chlorophenyl)boronic acid (70 mg, 0.45 mmol), K_2CO_3 (186 mg, 1.35 mmol) and $Pd(PPh_3)_3$ (26 mg, 0.02 mmol, 5 mol%) were reacted in dioxanne (3 mL) and water (1 mL) according to the general procedure for the Suzuki cross-couplings. Flash column chromatography afforded compound **50** (33 mg, 27%) as a brown foam. IR (neat): 3055, 2925, 1634, 1578, 1598, 1460, 1269, 1034 cm^{-1}. ^{1}H NMR (300 MHz, $CDCl_3$) δ 8.17 (s, 1H), 7.55 – 7.15 (m, 6H), 7.12 (dd, *J* = 8.1, 1.6 Hz, 1H), 5.70 (s, 1H), 3.47 (q, *J* = 7.2 Hz, 1H), 1.20 (t, *J* = 7.2 Hz, 3H). ^{13}C NMR (75 MHz, $CDCl_3$) δ 155.2, 141.4, 137.4, 132.7, 132.2, 131.8, 129.9, 128.0, 126.7, 122.6, 113.2, 111.8, 38.2, 15.2. HRMS ESI-TOF [*M*+H]$^+$ *m/z* calcd for $C_{15}H_{15}{}^{35}ClN_4$ 272.0955. Found 272.0966.

***N*-Ethyl-6-(3-nitrophenyl)-1*H*-benzo[*d*]imidazol-2-amine (51)**

6-Bromo-*N*-ethyl-1*H*-benzo[*d*]imidazol-2-amine (108 mg, 0.45 mmol), (3-nitrophenyl)boronic acid (75 mg, 0.45 mmol), K_3PO_4 (286 mg, 1.35 mmol) and $PdCl_2$(dtbpf) (15 mg, 0.02 mmol, 5 mol%) were reacted in dioxanne and water according to the general procedure for the Suzuki cross-couplings. Flash column chromatography afforded compound **51** (21 mg, 16%) as a yellow foam. IR (neat): 3075, 2926, 1603, 1519, 1467, 1342, 1267, 1034 cm^{-1}. ^{1}H NMR (300 MHz, CD_3OD) δ 8.48 – 8.36 (m, 1H), 8.23 – 8.09 (m, 1H), 8.09 – 7.96 (m, 1H), 7.64 (dd, *J* = 16.3, 8.3 Hz, 1H), 7.57 (s, 1H), 7.50 – 7.33 (m, 2H), 3.49 (q, *J* =

7.2 Hz, 2H), 1.36 (t, *J* = 7.2 Hz, 2H). 2H missing due to chemical exchange. ^{13}C NMR (75 MHz, CD_3OD) δ 155.6, 150.2, 144.6, 140.3, 136.3, 134.1, 131.1, 129.2, 128.1, 122.4, 122.2, 113.2, 111.2, 38.8, 15.1. HRMS ESI-TOF $[M+H]^+$ *m/z* calcd. for $C_{15}H_{15}N_4O_2$ 283.1195. Found 283.1184.

_N_-Ethyl-6-(3-methoxyphenyl)-1_H_-benzo[_d_]imidazol-2-amine (52)

6-Bromo-*N*-ethyl-1*H*-benzo[*d*]imidazol-2-amine (108 mg, 0.45 mmol), (3-methoxyphenyl)boronic acid (68 mg, 0.45 mmol), K_3PO_4 (286 mg, 1.35 mmol) and $PdCl_2$(dtbpf) (15 mg, 0.02 mmol, 5 mol%) were reacted in dioxanne and water according to the general procedure for the Suzuki cross-couplings. Flash column chromatography afforded compound **52** (40 mg, 33%) as a light brown foam. IR (neat): 3386, 2931, 2833, 1635, 1575, 1465, 1269, 1220, 1163, 1047, 1023 cm^{-1}. ^{1}H NMR (300 MHz, $CDCl_3$) δ 7.51 (s, 1H), 7.42 – 7.24 (m, 3H), 7.24 – 7.08 (m, 2H), 6.90 – 6.78 (m, 1H), 6.35 (s, 1H), 5.19 (s, 1H), 3.83 (s, 3H), 3.48 (q, *J* = 7.2 Hz, 2H), 1.23 (t, *J* = 7.2 Hz, 3H). ^{13}C NMR (75 MHz, $CDCl_3$) δ 159.9, 155.8, 143.7, 137.9, 134.1, 126.6, 120.3, 119.7, 112.9, 112.4, 111.9, 110.6, 55.2, 38.1, 15.2. HRMS ESI-TOF $[M+H]^+$ *m/z* calcd. for $C_{16}H_{18}N_3O$ 268.1450. Found 268.1443.

_N_-Butyl-6-(3-nitrophenyl)-1_H_-benzo[_d_]imidazol-2-amine (53)

6-Bromo-*N*-butyl-1*H*-benzo[*d*]imidazol-2-amine (107 mg, 0.4 mmol), (3-nitrophenyl)boronic acid (67 mg, 0.4 mmol), K_3PO_4 (286 mg, 1.2 mmol) and $PdCl_2$(dtbpf) (14 mg, 0.02 mmol, 5 mol%) were reacted in dioxanne and water according to the general procedure for the Suzuki cross-couplings. Flash column chromatography afforded compound **53** (19 mg, 16%) as a yellow foam. IR (neat): 3392, 2927, 1635, 1600, 1581, 1524, 1463, 1344, 1270, 1099 cm^{-1}. ^{1}H NMR (300 MHz, Acetone-*d6*) δ 8.42 (t, *J* = 2.0 Hz, 1H), 8.17 – 7.98 (m, 2H), 7.69 (t, *J* = 8.0 Hz, 1H), 7.56 (d, *J* = 1.2 Hz, 1H), 7.42 – 7.22 (m, 2H), 6.41 (s, 1H), 3.49 (t, *J* = 7.1 Hz, 2H), 1.76 – 1.58 (m, 2H), 1.53 – 1.33 (m, 2H), 0.93 (t, *J* = 7.3 Hz, 3H). ^{13}C NMR (300 MHz, Acetone-*d6*) δ 157.5, 149.8, 145.2, 141.0, 140.4, 133.7, 130.8, 121.8, 121.4, 119.9, 113.0, 111.0, 43.3, 32.8, 20.7, 14.1. HRMS ESI-TOF $[M+H]^+$ *m/z* calcd for $C_{17}H_{19}N_4O_2$ 311.1508. Found 311.1513.

_N_-Butyl-6-(3-methoxyphenyl)-1_H_-benzo[_d_]imidazol-2-amine (54)

6-Bromo-*N*-butyl-1*H*-benzo[*d*]imidazol-2-amine (107 mg, 0.4 mmol), (3-methoxyphenyl)boronic acid (61 mg, 0.4 mmol), K_3PO_4 (255 mg, 1.2 mmol) and $PdCl_2$(dtbpf) (14 mg, 0.02 mmol, 5 mol%) were reacted in dioxanne and water according to the general procedure for the Suzuki cross-couplings. Flash column chromatography afforded compound **54** (61 mg, 52%) as a light brown foam. IR (neat): 3058, 2955, 1636, 1577, 1464, 1270, 1221, 1163, 1047, 1034 cm^{-1}. ^1H NMR (300 MHz, $CDCl_3$) δ 7.53 (s, 1H), 7.43 – 7.23 (m, 3H), 7.24 – 7.06 (m, 2H), 6.92 – 6.79 (m, 1H), 5.24 (s, 2H), 3.85 (s, 3H), 3.42 (t, J = 7.1 Hz, 2H), 1.61 (dt, J = 14.9, 7.4 Hz, 2H), 1.47 – 1.29 (m, 2H), 0.89 (t, J = 7.3 Hz, 3H). ^{13}C NMR (75 MHz, $CDCl_3$) δ 159.9, 155.4, 143.7, 137.4, 134.3, 129.6, 128.6, 120.4, 119.7, 112.8, 112.4, 111.9, 110.8, 55.2, 43.2, 31.9, 20.0, 13.7. HRMS ESI-TOF $[M+H]^+$ *m/z* calcd for $C_{18}H_{22}N_3O$ 296.1763. Found 296.1762.

_N_-Butyl-6-(thiophen-3-yl)-1_H_-benzo[_d_]imidazol-2-amine (55)

6-Bromo-*N*-butyl-1*H*-benzo[*d*]imidazol-2-amine (107 mg, 0.4 mmol), thiophen-3-ylboronic acid (51 mg, 0.4 mmol), K_3PO_4 (255 mg, 1.2 mmol) and $PdCl_2$(dtbpf) (14 mg, 0.02 mmol, 5 mol%) were reacted in dioxanne and water according to the general procedure for the Suzuki cross-couplings. Flash column chromatography afforded compound **55** (75 mg, 69%) as a light brown foam. IR (neat): 3389, 3100, 2927, 1634, 1575, 1459, 1363, 1271, 1229, 1032 cm^{-1}. ^1H NMR (300 MHz, $CDCl_3$) δ 7.55 (s, 1H), 7.48 (s, 1H), 7.39 – 7.29 (m, 5H), 5.15 (s, 1H), 3.43 (t, J = 7.1 Hz, 2H), 1.66 – 1.46 (m, 2H), 1.40 – 1.23 (m, 2H), 0.85 (t, J = 7.3 Hz, 3H). ^{13}C NMR (75 MHz, $CDCl_3$) δ 156.0, 143.2, 137.8, 129.0, 126.6, 125.9, 119.6, 118.8, 109.9, 43.1, 31.9, 20.0, 13.7. HRMS ESI-TOF $[M+H]^+$ *m/z* calcd. for $C_{15}H_{18}N_3S$ 272.1221. Found 272.1217.

_N_-Butyl-6-((trimethylsilyl)ethynyl)-1_H_-benzo[_d_]imidazol-2-amine (56)

A mixture of compound **32** (536 mg, 2 mmol, 1 equiv.), trimethylsilylacetylene (831 µL, 6 mmol, 3 equiv.) and triethylamine (836 µL, 6 mmol, 5 equiv.) in dry DMF (0.5 mL) was degassed under a flow of Argon for 5 minutes. $PdCl_2$(dtbpf) (68 mg, 0.1 mmol, 10 mol%) and CuI (38 mg, 0.2 mmol, 20 mol%) were then added and the reaction mixture was heated at 60°C for 16h. The reaction mixture was allowed to cool to room temperature then concentrated under reduced pressure. The crude was purified by flash column chromatography on silica gel (CH_2Cl_2/CH_3OH : 95/5) to afford compound **56** (324 mg, 57%)

as a brown foam. ^{1}H NMR (300 MHz, $CDCl_3$) δ 9.54 (s, 1H), 7.45 – 6.58 (m, 3H), 5.29 (s, 1H), 3.49 – 2.90 (m, 2H), 1.48 – 1.15 (m, 2H), 1.13 – 0.78 (m, 2H), 0.70 – 0.34 (m, 3H), -0.03 (s, 9H). ^{13}C NMR (75 MHz, $CDCl_3$) δ 156.5, 138.4, 136.4, 125.4, 114.8, 111.8, 106.4, 91.6, 84.8, 42.9, 31.7, 19.8, 13.5, 0.0. HRMS ESI-TOF $[M+H]^+$ *m/z* calcd. For $C_{16}H_{24}N_3{}^{28}Si$ 286.1740. Found 286.1752.

***N*-Butyl-6-ethynyl-1*H*-benzo[*d*]imidazol-2-amine (57)**

Compound **56** (251 mg, 0.88 mmol) and K_2CO_3 (134 mg, 0.97 mmol) were reacted in MeOH/water : 1/1 (1 mL) at room temperature for 16h. The reaction mixture was then concentrated under reduced pressure. The crude was purified by flash column chromatography on silica gel (CH_2Cl_2/CH_3OH: 95/5) to afford compound **57** (140 mg, 86%) as a yellow foam. IR (neat): 3397, 3285, 2957, 2102, 1632, 1593, 1571, 1462, 1273, 1218, 1118 cm^{-1}. ^{1}H NMR (300 MHz, $CDCl_3$) δ 7.35 (s, 1H), 7.33 – 7.14 (m, 2H), 5.34 (s, 1H), 5.10 (s, 1H), 3.41 (t, *J* = 7.1 Hz, 2H), 3.00 (s, 1H), 1.79 – 1.48 (m, 2H), 1.45 – 1.23 (m, 2H), 0.89 (t, *J* = 7.3 Hz, 3H). ^{13}C NMR (75 MHz, $CDCl_3$) δ 156.1, 139.7, 136.9, 125.6, 115.4, 113.7, 112.4, 85.0, 75.0, 43.1, 20.0, 13.7.

6-(1-Benzyl-1H-1,2,3-triazol-4-yl)-N-ethyl-1H-benzo[d]imidazol-2-amine (58)

A mixture of benzyl bromide (52 µL, 0.44 mmol, 1.1 equiv.), NaN_3 (29 mg, 0.44 mmol, 1.1 equiv.) was stirred in DMF (0.5 mL) and water (0.1 mL) at room temperature for 16h. Once the intermediate azide is formed (TLC control using Heptane/EtOAc : 8/2), compound **57** (85 mg, 0.40 mmol, 1 equiv.), $CuSO_4.5H_2O$ (10 mg, 0.04 mmol, 10 mol%) and sodium ascorbate (16 mg, 0.08 mmol, 20 mol%) were added. The reaction mixture was stirred for further 16h at room temperature. Afterward, the reaction mixture was concentrated under reduced pressure and the crude purified by flash column chromatography on silica gel (CH_2Cl_2/CH_3OH: 95/5) to afford compound **58** (56 mg, 40%) as a brown foam. IR (neat): 3031, 2926, 2164, 1671, 1456, 1222, 1071 cm^{-1}. ^{1}H NMR (300 MHz, CD_3OD) δ 8.39 – 8.24 (m, 1H), 7.77 (s, 1H), 7.60 (t, *J* = 10.9 Hz, 1H), 7.43 – 7.29 (m, 6H), 5.62 (s, 2H), 1.68 (dt, *J* = 14.4, 7.0 Hz, 2H), 1.55 – 1.35 (m, 2H), 0.99 (t, *J* = 7.3 Hz, 3H). 2H missing due to chemical exchange with

MeOD. ^{13}C NMR (75 MHz, CD_3OD) δ 153.7, 149.2, 136.8, 133.8, 133.6, 130.1, 129.6, 129.1, 126.7, 122.1, 121.8, 112.8, 109.5, 55.1, 44.1, 32.1, 21.0, 14.1. HRMS ESI-TOF $[M+H]^+$ *m/z* calcd For $C_{20}H_{23}N_6$ 347.1984. Found 347.1977.

4.1.4. General procedure for the amidation with 1,5,7-triazabicyclo[4.4.0]dec-5-ene (TBD)

Procedure A

A mixture of 2-aminobenzimidazole (limiting reagent) and triazabicyclodecene (TBD, 1 equiv.) was stirred in DMF (1 mL) until the formation of a heavy precipitate, then amine (1.2 equiv.) was added and the reaction mixture was at 90 °C for 16 h under air. After, the reaction mixture was evaporated to remove volatiles. The residue was either purified by flash column chromatography on silica gel (CH_2Cl_2/CH_3OH : 95/5).

Procedure B

A mixture of 2-aminobenzimidazole (limiting reagent), triazabicyclodecene (TBD, 1 equiv.) and amine (5 equiv.) was stirred at 90 °C for 16 h under air. After, the reaction mixture was evaporated to remove volatiles. The residue was either purified by flash column chromatography on silica gel (CH_2Cl_2/CH_3OH : 95/5).

***N*-Ethyl-2-((6-nitro-1*H*-benzo[*d*]imidazol-2-yl)amino)acetamide (59)**

Ethyl (6-nitro-1*H*-benzo[*d*]imidazol-2-yl)glycinate (70 mg, 0.3 mmol), triazabicyclodecene (42 mg, 0.3 mmol) and ethylamine (100 µL, 1.5 mmol, 5 equiv.) were reacted according to the procedure B. Flash column chromatography afforded compound **59** (54 mg, 62%) as a orange amorphous solid. IR (neat): 3363, 3240, 2922, 1673, 1615, 1515, 1451, 1329, 1242, 1122, 1042 cm^{-1}. ^1H NMR (300 MHz, Acetone-*d6*) δ 8.04 (d, J = 2.3 Hz, 1H), 7.93 (dd, J = 8.7, 2.3 Hz, 1H), 7.51 (s, 1H), 7.28 (d, J = 8.7 Hz, 1H), 6.88 (s, 1H), 4.15 (s, 2H), 3.32 – 3.22 (m, 1H), 1.10 (t, J = 7.2 Hz, 3H). ^{13}C NMR (75 MHz, Acetone-*d6*) δ 169.7, 159.3, 144.1, 142.0, 139.2, 139.4, 117.6, 112.8, 107.9, 46.5, 34.7, 15.1. HRMS ESI-TOF $[M+H]^+$ *m/z* calcd For $C_{11}H_{14}N_5O_3$ 264.1097. Found: 264.1106.

***N*-Butyl-2-((6-nitro-1*H*-benzo[*d*]imidazol-2-yl)amino)acetamide (60)**

Ethyl (6-nitro-1*H*-benzo[*d*]imidazol-2-yl)glycinate (70 mg, 0.3 mmol), triazabicyclodecene (42 mg, 0.3 mmol) and *n*-butylamine (148 µL, 1.5 mmol, 5 equiv.) were reacted according to the procedure B for the amidation. Flash column chromatography afforded compound **60** (37 mg, 42%) as a yellow amorphous solid. IR (neat): 3267, 2956, 2928, 1592, 1530, 1461, 1279, 1092 cm^{-1}. ^{1}H NMR (300 MHz, Acetone-*d6*) δ 10.71 (s, 1H), 8.06 (d, J = 2.2 Hz, 1H), 7.94 (s, 1H), 7.47 (s, 1H), 7.29 (d, J = 8.8 Hz, 1H), 6.84 (s, 1H), 4.14 (s, 2H), 3.40 – 3.09 (m, 2H), 1.57 – 1.42 (m, 2H), 1.40 – 1.15 (m, 2H), 0.89 (t, J = 7.2 Hz, 3H). ^{13}C NMR (75 MHz, Acetone-*d6*) δ 168.3, 157.8, 146.5, 143.7, 139.7, 119.4, 114.0, 109.3, 46.6, 39.5, 32.4, 20.6, 14.0. HRMS ESI-TOF $[M+H]^+$ *m/z* calcd. For $C_{13}H_{18}N_5O_3$ 292.140. Found: 292.1407.

_N_-Benzyl-2-(butylamino)-1*H*-benzo[*d*]imidazole-6-carboxamide (61)

2-(Butylamino)-1*H*-benzo[*d*]imidazole-6-carboxylate (74 mg, 0.3 mmol), triazabicyclodecene (42 mg, 0.3 mmol) and benzylamine (68 µL, 1.5 mmol, 5 equiv.) were reacted according to the procedure B for the amidation. Flash column chromatography afforded compound **61** (62mg, 64%) as a white foam. IR (neat): 3256, 2925, 1606, 1562, 1460, 1280, 1218, 1026 cm^{-1}. ^{1}H NMR (300 MHz, DMSO-*d6*) δ 10.90 (s, 1H), 8.78 (t, J = 6.0 Hz, 1H), 7.69 (s, 1H), 7.51 (s, 1H), 7.41 – 7.23 (m, 4H), 7.28 – 7.16 (m, 1H), 7.12 (d, J = 8.2 Hz, 1H), 6.79 (s, 1H), 4.47 (d, J = 6.0 Hz, 2H), 3.33 – 3.19 (m, 2H), 1.56 (dt, J = 14.8, 7.3 Hz, 2H), 1.45 – 1.26 (m, 2H), 0.91 (t, J = 7.3 Hz, 3H). ^{13}C NMR (75 MHz, DMSO-*d6*) δ 167.07, 157.07, 140.2, 128.1, 127.1, 126.5, 119.8, 113.2, 107.9, 42.5, 41.9, 31.5, 19.5, 13.7. HRMS ESI-TOF $[M+H]^+$ *m/z* calcd For $C_{19}H_{23}N_4O$ 323.1872. Found 323.1862.

Methyl 2-(butylamino)-1*H*-benzo[*d*]imidazole-6-carboxylate (62)

2-(Butylamino)-1*H*-benzo[d]imidazole-6-carboxylate (111 mg, 0.45 mmol), triazabicyclodecene (63 mg, 0.45 mmol) and 2-phenylethylamine (68 µL, 0.45 mmol, 1.2 equiv.) were reacted according to the procedure A for the amidation. Flash column chromatography afforded compound **62** (21 mg, 14%) as a white foam. IR (neat): 3323, 3212, 2959, 1646, 1604, 1539, 1476, 1282, 1219, 1135, 1135 cm^{-1}. ^{1}H NMR (300 MHz, CD_3OD) δ 7.65 (d, J = 1.4 Hz, 1H), 7.46 (m, 1H), 7.39 – 7.13 (m, 6H), 3.71 – 3.52 (m, 2H), 3.48 – 3.35 (m, 2H), 3.02 – 2.86 (m, 2H), 1.74 – 1.56 (m, 2H), 1.56 – 1.38 (m, 2H), 1.00 (t, J = 7.3 Hz, 3H). 3H missing due to chemical exchange with MeOD. ^{13}C NMR (75 MHz, CD_3OD) δ

168.7, 154.7, 145.0, 141.3, 129.9, 129.5, 127.3, 121.1, 120.1, 155.0, 112.3, 111.6, 43.6, 42.7, 36.7, 33.0, 21.0, 13.9. HRMS ESI-TOF [*M*+H]$^+$ *m/z* calcd For $C_{20}H_{25}N_4O$ 337.2028. Found 337.2034.

2-(Butylamino)-*N*-(3-phenylpropyl)-1*H*-benzo[*d*]imidazole-6-carboxamide (63)

2-(Butylamino)-1*H*-benzo[*d*]imidazole-6-carboxylate (74 mg, 0.3 mmol), triazabicyclodecene (42 mg, 0.3 mmol) and 3-phenylpropylamine (213 µL, 1.5 mmol, 5 equiv.) were reacted according to the procedure B for the amidation. Flash column chromatography afforded compound **63** (48 mg, 46%) as a pink foam. IR (neat): 3267, 2956, 2928, 1592, 1530, 1461, 1279, 1092 cm^{-1}. ^{1}H NMR (300 MHz, CD_3OD) δ 7.69 (d, J = 1.6 Hz, 1H), 7.51 (dd, J = 8.3, 1.7 Hz, 1H), 7.30 – 7.04 (m, 6H), 3.48 – 3.26 (m, 4H), 2.75 – 2.58 (m, 2H), 2.00 – 1.81 (m, 2H), 1.71 – 1.52 (m, 2H), 1.51 – 1.33 (m, 2H), 0.97 (t, J = 7.3 Hz, 3H). 3H missing due to chemical exchange with MeOD. ^{13}C NMR (75 MHz, CD_3OD) δ 171.3, 158.5, 143.1, 129.4, 127.5, 126.9, 121.1, 112.4, 111.6, 43.6, 40.8, 34.4, 33.0, 32.5, 21.1, 14.2. HRMS ESI-TOF [*M*+H]$^+$ *m/z* calcd. For $C_{21}H_{27}N_4O$ 351.2185. Found 351.2168.

4.1.5. General procedure for the synthesis of the 2-aminobenzothiazoles 66 and (67) [23]

A mixture of the corresponding 2-chloro-6-nitrobenzo[*d*]thiazole **64** or 2-chloro-5-nitrobenzo[*d*]thiazole **65** (429, mg, 2 mmol), DBU (30 µL, 0.2 mmol, 10 mol%), $NaHCO_3$ (190 mg, 1.8 mmol, 0.9 equiv.) was vigorously stirred with a spatula then left on standing for 5 minutes until the reaction mixture became a thick solid. The resulting solid was washed with water and then recrystallized from ethanol.

***N*-Butyl-6-nitrobenzo[*d*]thiazol-2-amine (66)**

2-Chloro-6-nitrobenzo[*d*]thiazole (429 mg, 2 mmol, DBU (30 µL, 0.2 mmol, 10 mol%), $NaHCO_3$ (190 mg, 1.8 mmol, 0.9 equiv.) were reacted following the general procedure for the synthesis of the 2-aminobenzothiazoles. Recrystallization from ethanol afforded compound **66** (303 mg, 60%) as a yellow solid. IR (neat): 3096, 2957, 2862, 1624, 1562, 1456, 1328, 1286, 1214, 1124, 1037 cm^{-1}. ^{1}H NMR (300 MHz, $CDCl_3$) δ 8.50 (t, J = 2.6 Hz, 1H), 8.27 – 8.10 (m, 1H), 7.46 (dd, J = 8.9, 2.8 Hz, 1H), 6.78 (s, 1H), 3.46 (td, J = 7.1, 2.7 Hz, 2H), 1.72 (qd, J

= 7.7, 2.6 Hz, 2H), 1.54 – 1.31 (m, 2H), 0.97 (td, *J* = 7.3, 2.8 Hz, 3H). ^{13}C NMR (75 MHz, $CDCl_3$) δ 171.8, 157.6, 141.8, 130.4, 122.6, 117.6, 117.4, 45.8, 31.3, 20.0, 13.6. HRMS ESI-TOF [*M*+H]$^+$ *m/z* calcd For $C_{11}H_{14}N_3O_2S$ 252.0807. Found: 252.0804.

***N*-Butyl-5-nitrobenzo[*d*]thiazol-2-amine (67)**

2-Chloro-5-nitrobenzo[*d*]thiazole (429 mg, 2 mmol), DBU (30 µL, 0.2 mmol, 10 mol%), $NaHCO_3$ (190 mg, 1.8 mmol, 0.9 equiv.) were reacted following the general procedure for the synthesis of the 2-aminobenzothiazoles. Recrystallization from ethanol afforded **(67)** (294 mg, 58%) as a brown solid. IR (neat): 3010, 2855, 1611, 1504, 1329, 1290, 1080, 1058, 944 cm^{-1}. ^{1}H NMR (300 MHz, $CDCl_3$) δ 8.25 (d, *J* = 27.6 Hz, 1H), 7.96 (d, *J* = 8.6 Hz, 1H), 7.70 (d, *J* = 8.6 Hz, 1H), 6.77 (s, 1H), 3.47 (t, *J* = 7.1 Hz, 2H), 1.74 (dt, *J* = 14.8, 7.3 Hz, 2H), 1.48 (dq, *J* = 14.3, 7.3 Hz, 2H), 0.99 (t, *J* = 7.3 Hz, 3H). ^{13}C NMR (75 MHz, $CDCl_3$) δ 169.9, 153.1, 146.9, 120.8, 116.1, 113.2, 45.7, 31.5, 20.0, 13.7. HRMS ESI-TOF [*M*+H]$^+$ *m/z* calcd. For $C_{11}H_{14}N_3O_2S$ 252.0807. Found: 252.0801.

4.2. Biology

4.2.1. Cell cultures

The human cell lines FADD-deficient Jurkat I 2.1, Jurkat wild-type A3 and RPE-1 hTERT, were obtained from ATCC (American Type Culture Collection, Rockville, MD, USA). Jurkat wild type, FADD deficient Jurkat cells were cultured in RPMI containing Glutamax (Invitrogen) supplemented with 15% FCS. RPE-1 hTERT cells were cultured in DMEM-F12 containing Glutamax (Invitrogen) supplemented with 10% FCS. All cells were cultured under a 5% CO_2 atmosphere at 37 °C.

4.2.2. Reagents

Recombinant human Flag-tagged TRAIL (TRAIL-Flag) and z-VAD-fmk were obtained from Enzo Life Sciences (Villeurbanne, France). Necrostatin-1s (Nec-1s) were from Calbiochem (VWR International, Fontenay-sous-Bois, France). Sibiriline (Sib) was a kind gift of

SeaBeLife Biotech SAS (Roscoff, France). The cytokine TNF-α used for the cell-based assay was obtained from Invitrogen (Carlsbad, CA, USA).

4.2.3. Cell-based assays

The cell-based screening assay used for the characterization of necroptosis inhibitors has been previously described in Delehouzé et al.[5] and Le Cann et al.[4] The cell-death by necroptosis was induced in Jurkat FADD-deficient cells by addition of 10 ng/ml of human recombinant TNF-α (Invitrogen). The chemical compounds tested here were formatted at 10 mM in 100% DMSO in 96-well plates. The quantification of the cell viability was used as the main parameter to detect bioactive compounds. The cell viability was evaluated by detection of MTS reduction according to the manufacturer's instructions (CellTiter 96® AQueous Non-Radioactive Cell Proliferation Assay, Promega, Fitchburg, WI, USA) (see Delehouzé et al.[5] for experimental details). As the reduction of tetrazolium reagents can be occasionally observed under conditions in which cell death does not occur, we also used the lactate dehydrogenase (LDH) release assay, as independent cell death assay. The % of maximal cell death was determined by using the CyQUANT™ LDH Cytotoxicity Assay Kit (Invitrogen, Carlsbad, CA, USA), according to the manufacturer's instructions.

4.2.4. Protein kinase assays

Kinase enzymatic activities were assayed in 384-well plates using the ADP-Glo™ assay kit according the recommendations of the manufacturer (Promega, Madison, WI). This assay provides an homogeneous and high-throughput screening method to measure kinase activity by quantifying the amount of ADP produced during a kinase.[31] The reactions were carried in the presence of 10 µM ATP. The transmitted signal was measured using the Envision (PerkinElmer, Waltham, MA) microplate luminometer and expressed in Relative Light Unit (RLU). Peptide substrates were obtained from Proteogenix (Schiltigheim, France). These experiments were performed on the Kinase Inhibitor Specialized Screening facility (KISSf, FR2424, Station Biologique, Roscoff, France).

The following **buffers** were used: **(A)** 10 mM $MgCl_2$, 1 mM EGTA, 1 mM DTT, 25 mM Tris-HCl pH 7.5, 50 µg/ml heparin; **(B)** 25 mM MOPS, pH7.2, 12.5 mM β-glycerophosphate, 25 mM $MgCl_2$, 5 mM EGTA, 2 mM EDTA, 0.25 mM DTT; **(C)** 5 mM MOPS pH 7.2, 2.5 mM β-

glycerophosphate, 4 mM $MgCl_2$, 2.5 mM $MnCl_2$, 1 mM EGTA, 0.5 mM EDTA, 50 µg/ml BSA, 0.05 mM DTT.

The following **protein kinases** were analyzed during this study: **AuroraB** (human, recombinant, expressed by baculovirus in Sf9 insect cells, SignalChem, product #A31-10G) was assayed in buffer B with 0.16 µg/µl of myelin basic protein (MBP) as substrate; **CDK2/ CyclinA** (cyclin-dependent kinase-2, human, kindly provided by Dr. A. Echalier-Glazer, Leicester, UK) was assayed in buffer A with 0.8 µg/µl of histone H1 as substrate; **CDK5/p25** (human, recombinant, expressed in bacteria) was assayed in buffer A with 0.8 µg/µl of histone H1 as substrate; **CDK9/CyclinT** (human, recombinant, expressed by baculovirus in Sf9 insect cells) was assayed in buffer A with 0.27 µg/µl of the following peptide: YSPTSPSYSPTSPSYSPTSPSKKKK, as substrate; **CK1ε** (human, recombinant, expressed by baculovirus in Sf9 insect cells) was assayed in buffer A with 0.022 µg/µl of the following peptide: RRKHAAIGSpAYSITA ("Sp" stands for phosphorylated serine) as CK1-specific substrate; **HASPIN-kd** (human, kinase domain, amino acids 470 to 798, recombinant, expressed in bacteria) was assayed in buffer A with 0.007 µg/µl of Histone H3 (1-21) peptide (ARTKQTARKSTGGKAPRKQLA) as substrate; **Pim-1** (human proto-oncogene, recombinant, expressed in bacteria) was assayed in buffer A with 0.083µg/µl of histone H1 (Sigma #H5505) as substrate; **RIPK3** (human, recombinant, expressed by baculovirus in Sf9 insect cells) was assayed in buffer C with 0.1 µg/µl of MBP as substrate; ***Mm*CLK1** (from *Mus musculus*, recombinant, expressed in bacteria) was assayed in buffer A with 0.017 µg/µl of the following peptide: GRSRSRSRSRSR as substrate; ***Rn*DYRK1A-kd** (*Rattus norvegicu*s, amino acids 1 to 499 including the kinase domain, recombinant, expressed in bacteria, DNA vector kindly provided by Dr. W. Becker, Aachen, Germany) was assayed in buffer A with 0.033 µg/µl of the following peptide: KKISGRLSPIMTEQ as substrate; **ABL1** (human, amino acids 118 to 535, recombinant, expressed by baculovirus in Sf9 insect cells) were assayed in buffer A with 0.17 µg/µl of the following peptide (dubbed ABLtide): EAIYAAPFAKKK as ABL1-selective substrate; **JAK3** (human, C-terminal fragment, amino acids 781-1124, recombinant, expressed by baculovirus in Sf9 insect cells) were assayed in buffer A with 0.17 µg/µl of the following peptide (dubbed JAK3tide): GGEEEEYFELVKKKK as JAK3-selective substrate.

To validate each kinase assay, the following model inhibitors were used under the same conditions than the tested compounds: Barasertib (AZD1152-HQPA, #S1147, Selleckchem) for AuroraB; Staurosporine from *Streptomyces sp*. (#S5921, purity ≥95%, Sigma-Aldrich) for CK1ε; Indirubin-3'-oxime (#I0404, Sigma-Aldrich) for CDK2/CyclinA, CDK5/p25, CDK9/ CyclinT, *Rn*DYRK1A and *Mm*CLK1; CHR-6494 (#SML0648, Sigma-Aldrich) for HASPIN; Tofacitinib (CP-690550, #S2789, Selleckchem) for JAK3; Imatinib mesylate (STI571, #S1026, Selleckchem) for ABL1; GSK'872 (GSK2399872A, #S8465, Selleckchem) for RIPK3; SGI-1776 (#S2198, Selleckchem) for Pim1.

The catalytic activity of **RIPK1** was detected by Eurofins Discovery (Celle-L'Evescault, France) using a radiometric assay. Briefly, human RIPK1-kd (amino acids 8 to 322 including the kinase domain, recombinant) was assayed in 8 mM MOPS pH 7.0, 0.2 mM EDTA, 10 mM magnesium acetate with 0.33 mg/ml of MBP as substrate. The reaction was initiated by the addition of the Mg/[γ-^{33}P]ATP mix (155µM is the Km value used as ATP final concentration). After incubation for 120 minutes at room temperature, the reaction is stopped by the addition of phosphoric acid to a concentration of 0.5%. 10 µl of the stopped reaction is spotted onto a P30 filtermat and washed four times for 4 minutes in 0.425% phosphoric acid and once in methanol prior to drying and scintillation counting. This assay was validated using the Cdk1/2 Inhibitor III (CAS 443798-55-8) as control inhibitor.

4.3. Molecular docking

Three-dimensional structures of ligands were generated using CORINA 4.2.0 (http:// www.molecular-networks.com). Two tautomers were considered for the benzimidazole core of each ligand. Molecular docking calculations were carried out using GOLD software [32] and GoldScore scoring function, with the structure of RIPK1 (PDB code 6C3E) [14] as receptor. This structure was selected considering the similarity of the ligand with the structures reported in our study, as well as the conformation of residues Met67, Met92 and Phe162 in the binding pocket. The chain A of this structure was used, the missing loops and atoms being completed using MODELLER.[33] The binding site was defined as a sphere with 15 Å radius around the carbonyl oxygen of Asp156. In agreement with our previous studies [34–40] showing that an enhanced conformational search is beneficial, especially for large

molecules, a search efficiency of 200 % was used to better explore the ligand conformational space. All other parameters were used with the default values and 10 poses were generated for each ligand.

Molecular modeling images were generated using UCSF Chimera.[41]

Associated content

Supporting Information: copies of ^{1}H and ^{13}C NMR spectra and figures

Author contributions

Mohamed Benchekroun synthesized a part of compounds and co-wrote the manuscript.

Ludmila Ermolenko prepared some analogs

Minh Quan Tran and Agathe Vagneux: participated in the synthetic part

Claire Delehouzé, Mohamed Souab, Blandine Baratte et Béatrice Josselin: performed the experiments.

Claire Delehouzé, Sandrine Ruchaud and Stéphane Bach, analyzed the results

Stéphane Bach, supervised the screening and biological evaluation, co-wrote the manuscript.

Hristo Nedev carried out the molecular modeling experiments and analyzed the results

Bogdan I. Iorga, analyzed the molecular modeling results and co-wrote the manuscript.

Ali Al-Mourabit conceived and directed the project, supervised the findings of this work and wrote the manuscript.

E-mail addresses: bach@sb-roscoff.fr (S. Bach), ali.almourabit@cnrs.fr (A. Al-Mourabit)

Acknowlegdements

Financial support from CNRS is gratefully acknowledged.

The authors thank the Cancéropôle Grand-Ouest ("Marines Molecules, Metabolism and Cancer" network), IBiSA (French Infrastructures en sciences du vivant: biologie, santé et agronomie) and Biogenouest (Western France life science and environment core facility network) for supporting the KISSf screening facility, FR2424 (Roscoff, France). S. Bach is supported by ANR/Investissements d'Avenir program via the OCEANOMICs project (grant #ANR-11-BTBR-0008) and INCa ("NECROTRAIL" Program).

Conflict of Interest

Claire Delehouzé and Stéphane Bach are founders and members of the scientific advisory board of SeaBeLife Biotech (Roscoff, France). This company is developing novel therapies for treating liver and kidney acute disorders. Research in Roscoff was conducted in the absence of any commercial relationships that could be construed as a potential conflict of interest.

References

[1] R.A. Lockshin, C.M. Williams, Programmed cell death—II. Endocrine potentiation of the breakdown of the intersegmental muscles of silkmoths, J. Insect Physiol. 10 (1964) 643–649. https://doi.org/10.1016/0022-1910(64)90034-4.

[2] L. Galluzzi, I. Vitale, S.A. Aaronson, J.M. Abrams, D. Adam, P. Agostinis, E.S. Alnemri, L. Altucci, I. Amelio, D.W. Andrews, M. Annicchiarico-Petruzzelli, A.V. Antonov, E. Arama, E.H. Baehrecke, N.A. Barlev, N.G. Bazan, F. Bernassola, M.J.M. Bertrand, K. Bianchi, M.V. Blagosklonny, K. Blomgren, C. Borner, P. Boya, C. Brenner, M. Campanella, E. Candi, D. Carmona-Gutierrez, F. Cecconi, F.K.-M. Chan, N.S. Chandel, E.H. Cheng, J.E. Chipuk, J.A. Cidlowski, A. Ciechanover, G.M. Cohen, M. Conrad, J.R. Cubillos-Ruiz, P.E. Czabotar, V. D'Angiolella, T.M. Dawson, V.L. Dawson, V.D. Laurenzi, R.D. Maria, K.-M. Debatin, R.J. DeBerardinis, M. Deshmukh, N.D. Daniele, F.D. Virgilio, V.M. Dixit, S.J. Dixon, C.S. Duckett, B.D. Dynlacht, W.S. El-Deiry, J.W. Elrod, G.M. Fimia, S. Fulda, A.J. García-Sáez, A.D. Garg, C. Garrido, E. Gavathiotis, P. Golstein, E. Gottlieb, D.R. Green, L.A. Greene, H. Gronemeyer, A. Gross, G. Hajnoczky, J.M. Hardwick, I.S. Harris, M.O. Hengartner, C. Hetz, H. Ichijo, M. Jäättelä, B. Joseph, P.J. Jost, P.P. Juin, W.J. Kaiser, M. Karin, T. Kaufmann, O. Kepp, A. Kimchi, R.N. Kitsis, D.J. Klionsky, R.A. Knight, S. Kumar, S.W. Lee, J.J. Lemasters, B. Levine, A. Linkermann, S.A. Lipton, R.A. Lockshin, C. López-Otín, S.W. Lowe, T. Luedde, E. Lugli, M. MacFarlane, F. Madeo, M. Malewicz, W. Malorni, G. Manic, J.-C. Marine, S.J. Martin, J.-C. Martinou, J.P. Medema, P. Mehlen, P. Meier, S. Melino, E.A. Miao, J.D. Molkentin, U.M. Moll, C. Muñoz-Pinedo, S. Nagata, G. Nuñez, A. Oberst, M. Oren, M. Overholtzer, M. Pagano, T. Panaretakis, M. Pasparakis, J.M. Penninger, D.M. Pereira, S. Pervaiz, M.E. Peter, M. Piacentini, P. Pinton, J.H.M. Prehn, H. Puthalakath, G.A. Rabinovich, M. Rehm, R. Rizzuto, C.M.P. Rodrigues, D.C. Rubinsztein, T. Rudel, K.M. Ryan, E. Sayan, L. Scorrano, F. Shao, Y. Shi, J. Silke, H.-U. Simon, A. Sistigu, B.R. Stockwell, A. Strasser, G. Szabadkai, S.W.G. Tait, D. Tang, N. Tavernarakis, A. Thorburn, Y. Tsujimoto, B. Turk, T.V. Berghe, P. Vandenabeele, M.G.V. Heiden, A. Villunger, H.W. Virgin, K.H. Vousden, D. Vucic, E.F. Wagner, H. Walczak, D. Wallach, Y. Wang, J.A. Wells, W. Wood, J. Yuan, Z. Zakeri, B. Zhivotovsky, L. Zitvogel, G. Melino, G. Kroemer, Molecular mechanisms of cell death: recommendations of the Nomenclature Committee on Cell Death 2018, Cell Death Differ. 25 (2018) 486–541. https://doi.org/10.1038/s41418-017-0012-4.

[3] S. Jouan-Lanhouet, M.I. Arshad, C. Piquet-Pellorce, C. Martin-Chouly, G. Le Moigne-Muller, F. Van Herreweghe, N. Takahashi, O. Sergent, D. Lagadic-Gossmann, P.

Vandenabeele, M. Samson, M.-T. Dimanche-Boitrel, TRAIL induces necroptosis involving RIPK1/RIPK3-dependent PARP-1 activation, Cell Death Differ. 19 (2012) 2003–2014. https://doi.org/10.1038/cdd.2012.90.

[4] F. Le Cann, C. Delehouzé, S. Leverrier-Penna, A. Filliol, A. Comte, O. Delalande, N. Desban, B. Baratte, I. Gallais, C. Piquet-Pellorce, F. Faurez, M. Bonnet, Y. Mettey, P. Goekjian, M. Samson, P. Vandenabeele, S. Bach, M.-T. Dimanche-Boitrel, Sibiriline, a new small chemical inhibitor of receptor-interacting protein kinase 1, prevents immune-dependent hepatitis, FEBS J. 284 (2017) 3050–3068. https://doi.org/10.1111/febs.14176.

[5] C. Delehouzé, S. Leverrier-Penna, F.L. Cann, A. Comte, M. Jacquard-Fevai, O. Delalande, N. Desban, B. Baratte, I. Gallais, F. Faurez, M.C. Bonnet, M. Hauteville, P.G. Goekjian, R. Thuillier, F. Favreau, P. Vandenabeele, T. Hauet, M.T. Dimanche-Boitrel, S. Bach, 6E11, a highly selective inhibitor of Receptor-Interacting Protein Kinase 1, protects cells against cold hypoxia-reoxygenation injury, Sci. Rep. 7 (2017) 12931. https://doi.org/10.1038/s41598-017-12788-4.

[6] W. Zhou, J. Yuan, Necroptosis in health and diseases, Semin. Cell Dev. Biol. 35 (2014) 14–23. https://doi.org/10.1016/j.semcdb.2014.07.013.

[7] A. Degterev, Z. Huang, M. Boyce, Y. Li, P. Jagtap, N. Mizushima, G.D. Cuny, T.J. Mitchison, M.A. Moskowitz, J. Yuan, Chemical inhibitor of nonapoptotic cell death with therapeutic potential for ischemic brain injury, Nat. Chem. Biol. 1 (2005) 112. https://doi.org/10.1038/nchembio711.

[8] P. Vandenabeele, S. Grootjans, N. Callewaert, N. Takahashi, Necrostatin-1 blocks both RIPK1 and IDO: consequences for the study of cell death in experimental disease models, Cell Death Differ. 20 (2013) 185–187. https://doi.org/10.1038/cdd.2012.151.

[9] X. Teng, A. Degterev, P. Jagtap, X. Xing, S. Choi, R. Denu, J. Yuan, G.D. Cuny, Structure–activity relationship study of novel necroptosis inhibitors, Bioorg. Med. Chem. Lett. 15 (2005) 5039–5044. https://doi.org/10.1016/j.bmcl.2005.07.077.

[10] C. Zhuang, F. Chen, Small-Molecule Inhibitors of Necroptosis: Current Status and Perspectives, J. Med. Chem. 63 (2020) 1490–1510. https://doi.org/10.1021/acs.jmedchem.9b01317.

[11] P.A. Harris, D. Bandyopadhyay, S.B. Berger, N. Campobasso, C.A. Capriotti, J.A. Cox, L. Dare, J.N. Finger, S.J. Hoffman, K.M. Kahler, R. Lehr, J.D. Lich, R. Nagilla, R.T. Nolte, M.T. Ouellette, C.S. Pao, M.C. Schaeffer, A. Smallwood, H.H. Sun, B.A. Swift, R.D. Totoritis, P. Ward, R.W. Marquis, J. Bertin, P.J. Gough, Discovery of Small Molecule RIP1 Kinase Inhibitors for the Treatment of Pathologies Associated with Necroptosis, ACS Med. Chem. Lett. 4 (2013) 1238–1243. https://doi.org/10.1021/ml400382p.

[12] P.A. Harris, B.W. King, D. Bandyopadhyay, S.B. Berger, N. Campobasso, C.A. Capriotti, J.A. Cox, L. Dare, X. Dong, J.N. Finger, L.C. Grady, S.J. Hoffman, J.U. Jeong, J. Kang, V. Kasparcova, A.S. Lakdawala, R. Lehr, D.E. McNulty, R. Nagilla, M.T. Ouellette, C.S. Pao, A.R. Rendina, M.C. Schaeffer, J.D. Summerfield, B.A. Swift, R.D. Totoritis, P. Ward, A. Zhang, D. Zhang, R.W. Marquis, J. Bertin, P.J. Gough, DNA-Encoded Library Screening Identifies Benzo[b][1,4]oxazepin-4-ones as Highly Potent and Monoselective Receptor Interacting Protein 1 Kinase Inhibitors, J. Med. Chem. 59 (2016) 2163–2178. https://doi.org/10.1021/acs.jmedchem.5b01898.

[13] K. Weisel, N.E. Scott, D.J. Tompson, B.J. Votta, S. Madhavan, K. Povey, A. Wolstenholme, M. Simeoni, T. Rudo, L. Richards−Peterson, T. Sahota, J.G. Wang, J.

Lich, J. Finger, A. Verticelli, M. Reilly, P.J. Gough, P.A. Harris, J. Bertin, M.-L. Wang, Randomized clinical study of safety, pharmacokinetics, and pharmacodynamics of RIPK1 inhibitor GSK2982772 in healthy volunteers, Pharmacol. Res. Perspect. 5 (2017) e00365. https://doi.org/10.1002/prp2.365.

[14] M. Yoshikawa, M. Saitoh, T. Katoh, T. Seki, S.V. Bigi, Y. Shimizu, T. Ishii, T. Okai, M. Kuno, H. Hattori, E. Watanabe, K.S. Saikatendu, H. Zou, M. Nakakariya, T. Tatamiya, Y. Nakada, T. Yogo, Discovery of 7-Oxo-2,4,5,7-tetrahydro-6H-pyrazolo[3,4-c]pyridine Derivatives as Potent, Orally Available, and Brain-Penetrating Receptor Interacting Protein 1 (RIP1) Kinase Inhibitors: Analysis of Structure–Kinetic Relationships, J. Med. Chem. (2018). https://doi.org/10.1021/acs.jmedchem.7b01647.

[15] S.B. Berger, P. Harris, R. Nagilla, V. Kasparcova, S. Hoffman, B. Swift, L. Dare, M. Schaeffer, C. Capriotti, M. Ouellette, B.W. King, D. Wisnoski, J. Cox, M. Reilly, R.W. Marquis, J. Bertin, P.J. Gough, Characterization of GSK'963: a structurally distinct, potent and selective inhibitor of RIP1 kinase., Cell Death Discov. 1 (2015) 15009–15009. https://doi.org/10.1038/cddiscovery.2015.9.

[16] P.A. Harris, N. Faucher, N. George, P.M. Eidam, B.W. King, G.V. White, N.A. Anderson, D. Bandyopadhyay, A.M. Beal, V. Beneton, S.B. Berger, N. Campobasso, S. Campos, C.A. Capriotti, J.A. Cox, A. Daugan, F. Donche, M.-H. Fouchet, J.N. Finger, B. Geddes, P.J. Gough, P. Grondin, B.L. Hoffman, S.J. Hoffman, S.E. Hutchinson, J.U. Jeong, E. Jigorel, P. Lamoureux, L.K. Leister, J.D. Lich, M.K. Mahajan, J. Meslamani, J.E. Mosley, R. Nagilla, P.M. Nassau, S.-L. Ng, M.T. Ouellette, K.K. Pasikanti, F. Potvain, M.A. Reilly, E.J. Rivera, S. Sautet, M.C. Schaeffer, C.A. Sehon, H. Sun, J.H. Thorpe, R.D. Totoritis, P. Ward, N. Wellaway, D.D. Wisnoski, J.M. Woolven, J. Bertin, R.W. Marquis, Discovery and Lead-Optimization of 4,5-Dihydropyrazoles as Mono-Kinase Selective, Orally Bioavailable and Efficacious Inhibitors of Receptor Interacting Protein 1 (RIP1) Kinase, J. Med. Chem. 62 (2019) 5096–5110. https://doi.org/10.1021/acs.jmedchem.9b00318.

[17] S. Pushpakom, F. Iorio, P.A. Eyers, K.J. Escott, S. Hopper, A. Wells, A. Doig, T. Guilliams, J. Latimer, C. McNamee, A. Norris, P. Sanseau, D. Cavalla, M. Pirmohamed, Drug repurposing: progress, challenges and recommendations, Nat. Rev. Drug Discov. 18 (2019) 41–58. https://doi.org/10.1038/nrd.2018.168.

[18] S. Hofmans, L. Devisscher, S. Martens, D. Van Rompaey, K. Goossens, T. Divert, W. Nerinckx, N. Takahashi, H. De Winter, P. Van Der Veken, V. Goossens, P. Vandenabeele, K. Augustyns, Tozasertib Analogues as Inhibitors of Necroptotic Cell Death, J. Med. Chem. (2018). https://doi.org/10.1021/acs.jmedchem.7b01449.

[19] S.B. Bharate, S.D. Sawant, P.P. Singh, R.A. Vishwakarma, Kinase Inhibitors of Marine Origin, Chem. Rev. 113 (2013) 6761–6815. https://doi.org/10.1021/cr300410v.

[20] S. Tilvi, C. Moriou, M.-T. Martin, J.-F. Gallard, J. Sorres, K. Patel, S. Petek, C. Debitus, L. Ermolenko, A. Al-Mourabit, Agelastatin E, Agelastatin F, and Benzosceptrin C from the Marine Sponge Agelas dendromorpha, J. Nat. Prod. 73 (2010) 720–723. https://doi.org/10.1021/np900539j.

[21] S. Wang, G. Dong, C. Sheng, Structural Simplification of Natural Products, Chem. Rev. (2019). https://doi.org/10.1021/acs.chemrev.8b00504.

[22] R. Frei, A.S. Breitbach, H.E. Blackwell, 2-Aminobenzimidazole Derivatives Strongly Inhibit and Disperse Pseudomonas aeruginosa Biofilms, Angew. Chem. Int. Ed. 51 (2012) 5226–5229. https://doi.org/10.1002/anie.201109258.

[23] S.K. Verma, B.N. Acharya, R. Ghorpade, A. Pratap, M.P. Kaushik, A DBU–diheteroaryl halide adduct as the fastest current N-diheteroarylating agent, RSC Adv. 3 (2013) 18783–18786. https://doi.org/10.1039/C3RA43179G.
[24] J. Hou, J. Ju, Z. Zhang, C. Zhao, Z. Li, J. Zheng, T. Sheng, H. Zhang, L. Hu, X. Yu, W. Zhang, Y. Li, M. Wu, H. Ma, X. Zhang, S. He, Discovery of potent necroptosis inhibitors targeting RIPK1 kinase activity for the treatment of inflammatory disorder and cancer metastasis, Cell Death Dis. 10 (2019) 1–13. https://doi.org/10.1038/s41419-019-1735-6.
[25] C.A. Belmokhtar, J. Hillion, E. Ségal-Bendirdjian, Staurosporine induces apoptosis through both caspase-dependent and caspase-independent mechanisms, Oncogene. 20 (2001) 3354–3362. https://doi.org/10.1038/sj.onc.1204436.
[26] F. Esser, P. Ehrengart, H.P. Ignatow, Cyclic guanidines. Part 6. 1 Synthesis of benzimidazoles by intramolecular vicarious nucleophilic substitution of hydrogen, J. Chem. Soc. Perkin 1. 0 (1999) 1153–1154. https://doi.org/10.1039/A900553F.
[27] G. Han, J. Ha Lee, M. Hyun An, E. Hyun Choi, H.-Y. Park Choo, A Facile Synthesis of 2-Acyl and 2-Alkylaminobenzimidazoles for 5-Lipoxygenase Inhibitors, Heterocycles. 70 (2006) 571. https://doi.org/10.3987/COM-06-S(W)25.
[28] X. Wang, L. Zhang, Y. Xu, D. Krishnamurthy, C.H. Senanayake, A practical synthesis of 2-(N-substituted)-aminobenzimidazoles utilizing CuCl-promoted intramolecular cyclization of N-(2-aminoaryl)thioureas, Tetrahedron Lett. 45 (2004) 7167–7170. https://doi.org/10.1016/j.tetlet.2004.07.042.
[29] PubChem, N-Cyclohexyl-6-methyl-1H-benzimidazol-2-amine, (2019). https://pubchem.ncbi.nlm.nih.gov/compound/71190137 (accessed August 6, 2019).
[30] PubChem, 6-Chloro-N-cyclohexyl-1H-benzimidazol-2-amine, (2019). https://pubchem.ncbi.nlm.nih.gov/compound/33697394 (accessed August 6, 2019).
[31] H. Zegzouti, M. Zdanovskaia, K. Hsiao, S.A. Goueli, ADP-Glo: A Bioluminescent and Homogeneous ADP Monitoring Assay for Kinases, ASSAY Drug Dev. Technol. 7 (2009) 560–572. https://doi.org/10.1089/adt.2009.0222.
[32] M.L. Verdonk, J.C. Cole, M.J. Hartshorn, C.W. Murray, R.D. Taylor, Improved protein–ligand docking using GOLD, Proteins Struct. Funct. Bioinforma. 52 (2003) 609–623. https://doi.org/10.1002/prot.10465.
[33] A. Šali, T.L. Blundell, Comparative Protein Modelling by Satisfaction of Spatial Restraints, J. Mol. Biol. 234 (1993) 779–815. https://doi.org/10.1006/jmbi.1993.1626.
[34] G. Surpateanu, B.I. Iorga, Evaluation of docking performance in a blinded virtual screening of fragment-like trypsin inhibitors, J. Comput. Aided Mol. Des. 26 (2012) 595–601. https://doi.org/10.1007/s10822-011-9526-x.
[35] C. Colas, B.I. Iorga, Virtual screening of the SAMPL4 blinded HIV integrase inhibitors dataset, J. Comput. Aided Mol. Des. 28 (2014) 455–462. https://doi.org/10.1007/s10822-014-9707-5.
[36] V.Y. Martiny, F. Martz, E. Selwa, B.I. Iorga, Blind Pose Prediction, Scoring, and Affinity Ranking of the CSAR 2014 Dataset, J. Chem. Inf. Model. 56 (2016) 996–1003. https://doi.org/10.1021/acs.jcim.5b00337.
[37] E. Selwa, V.Y. Martiny, B.I. Iorga, Molecular docking performance evaluated on the D3R Grand Challenge 2015 drug-like ligand datasets, J. Comput. Aided Mol. Des. 30 (2016) 829–839. https://doi.org/10.1007/s10822-016-9983-3.

[38] E. Selwa, E. Elisée, A. Zavala, B.I. Iorga, Blinded evaluation of farnesoid X receptor (FXR) ligands binding using molecular docking and free energy calculations, J. Comput. Aided Mol. Des. 32 (2018) 273–286. https://doi.org/10.1007/s10822-017-0054-1.
[39] L. Chaput, E. Selwa, E. Elisée, B.I. Iorga, Blinded evaluation of cathepsin S inhibitors from the D3RGC3 dataset using molecular docking and free energy calculations, J. Comput. Aided Mol. Des. 33 (2019) 93–103. https://doi.org/10.1007/s10822-018-0161-7.
[40] E. Elisée, V. Gapsys, N. Mele, L. Chaput, E. Selwa, B.L. de Groot, B.I. Iorga, Performance evaluation of molecular docking and free energy calculations protocols using the D3R Grand Challenge 4 dataset, J. Comput. Aided Mol. Des. 33 (2019) 1031–1043. https://doi.org/10.1007/s10822-019-00232-w.
[41] E.F. Pettersen, T.D. Goddard, C.C. Huang, G.S. Couch, D.M. Greenblatt, E.C. Meng, T.E. Ferrin, UCSF Chimera—A visualization system for exploratory research and analysis, J. Comput. Chem. 25 (2004) 1605–1612. https://doi.org/10.1002/jcc.20084.

Graphical Abstract

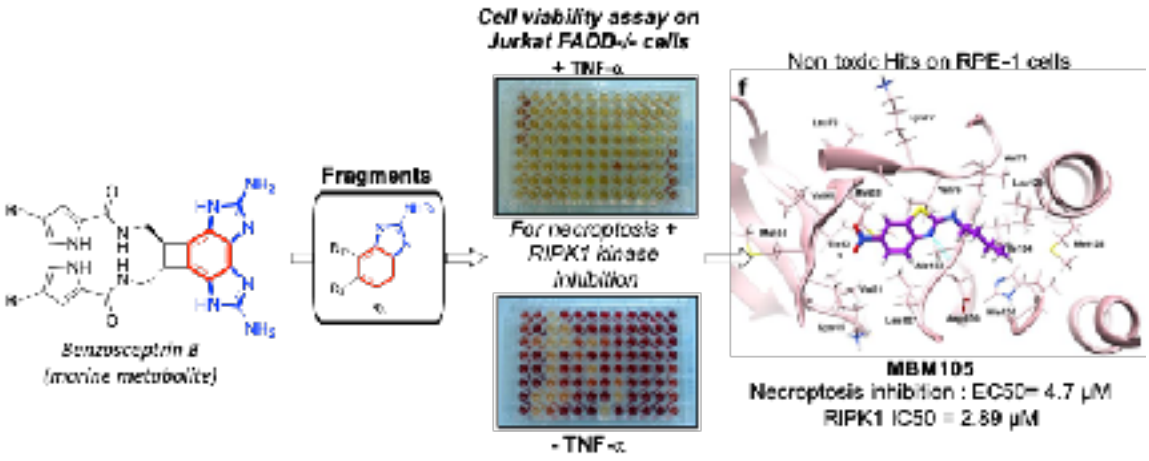

Graphical Abstract